Tomography of the Quark-Gluon-Plasma by Charm Quarks

Elena Bratkovskaya

In collaboration with Taesoo Song, Hamza Berrehrah, Daniel Cabrera, Juan Torres-Rincon, Laura Tolos, Wolfgang Cassing, Jörg Aichelin and Pol-Bernard Gossiaux

The Heavy Flavor Working Group Meeting,
Berkeley Lab., USA, 18-22 January 2016

Motivation

❑ study of the properties of hot and dense nuclear and partonic matter by ‚charm probes‘:

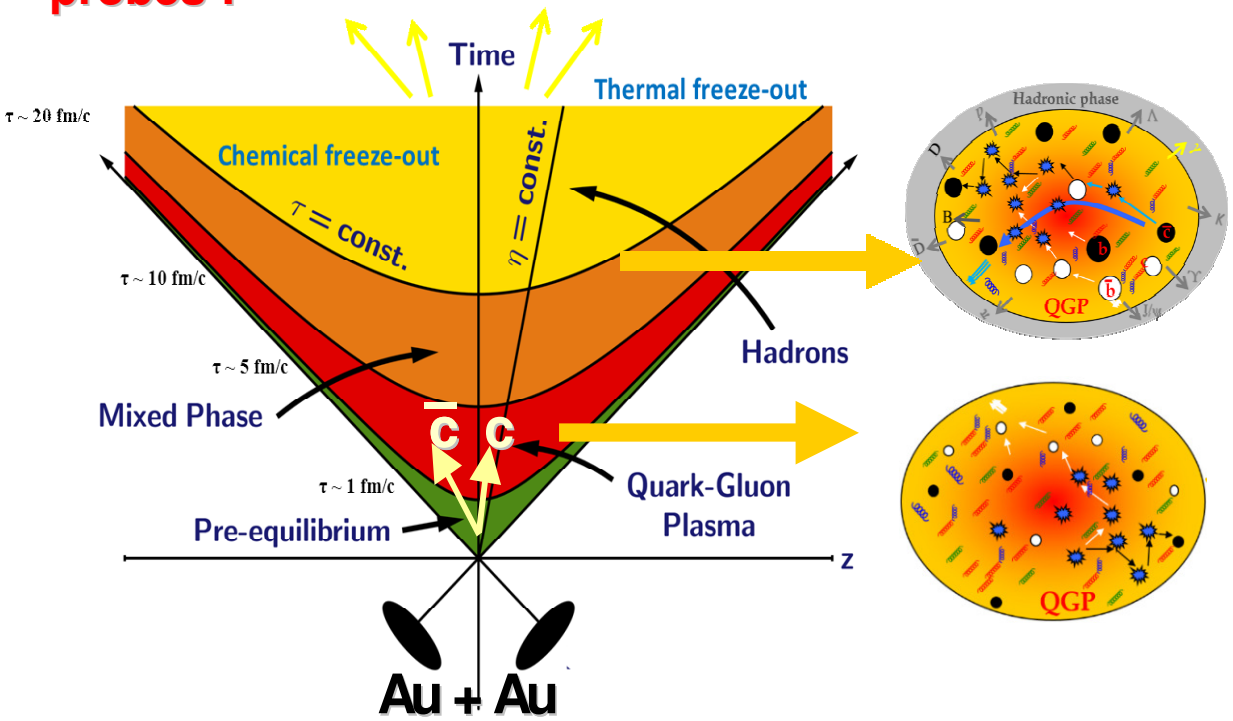

➔ Hope to use ’charm probes’ for an early tomography of the QGP

The advantages of the ’charm probes’:

❑ dominantly produced in the very early stages of the reactions in initial binary collisions with large energy-momentum transfer

❑ initial charm production is well described by pQCD – FONLL

❑ scattering cross sections are small (compared to the light quarks) ➔ not in an equilibrium with the surrounding matter

Charm: experimental signals

1. Nuclear modification factor:

$$R_{AA}(p_T) \equiv \frac{dN_D^{Au+Au}/dp_T}{N_{\text{binary}}^{Au+Au} \times dN_D^{p+p}/dp_T}$$

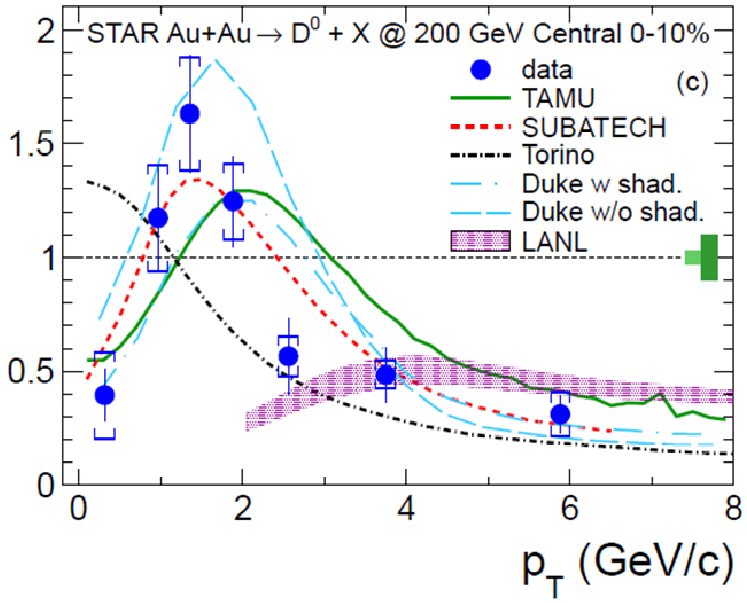

2. Elliptic flow v_2:

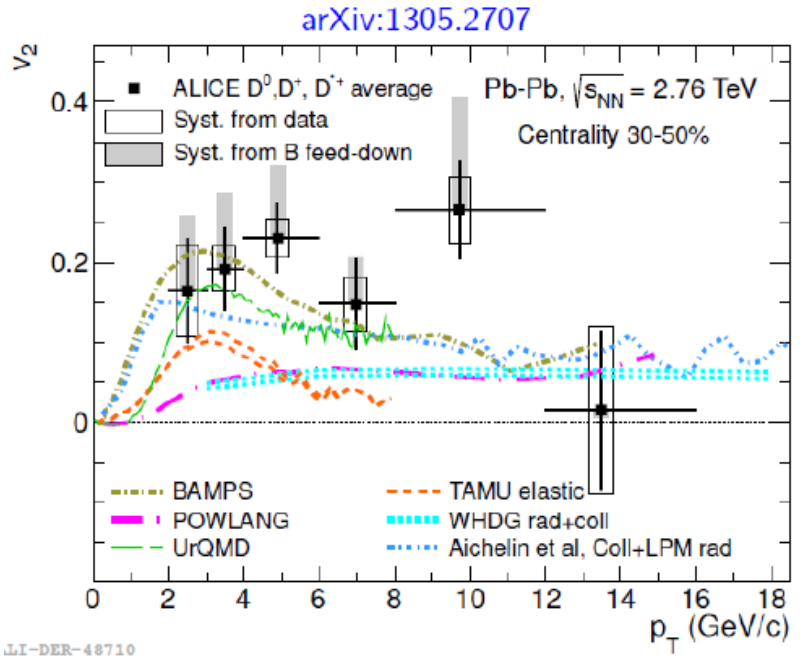

❑ **What is the origin for the "energy loss" of charm at large p_T?**

Collisional energy loss (elastic scattering Q+q→Q+q)
vs radiative (gluon bremsstrahlung Q+q→Q+q+g) ?

➔ **Challenge for theory: simultaneous description of R_{AA} and v_2 !**

Dynamics of charm quarks in A+A

1. **Production** of charm quarks in initial binary collisions

2. **Interactions in the QGP**:
   elastic scattering Q+q→Q+q ➔ **collisional** energy loss
   gluon bremsstrahlung Q+q→Q+q+g ➔ **radiative** energy loss

3. **Hadronization**: c/cbar quarks →D(D*)-mesons:
   coalescence vs fragmentation

4. **Hadronic interactions**:
   D+baryons; D+mesons

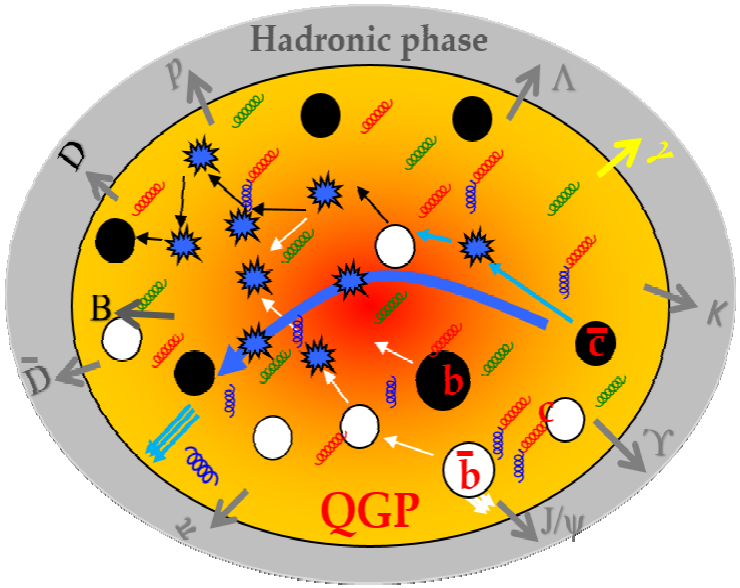

The goal: to model the dynamics of charm quarks/mesons in all phases on a **microscopic basis**

The tool: PHSD approach

Basic idea of PHSD

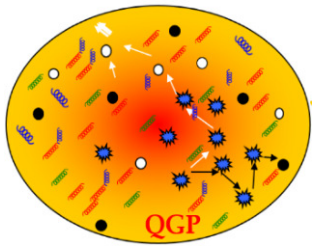

QGP in equilibrium

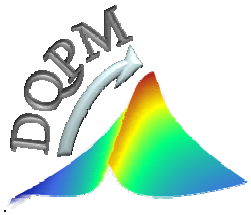

fitted to

IQCD

controled by IQCD!

Dynamical QuasiParticle Model (DQPM)

Quasiparticle properties: ‚resummed' self-energies, propagators
➔Calculation of cross sections

Calculation of transport coefficients η, ζ, σ_0

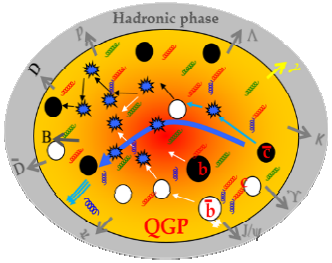

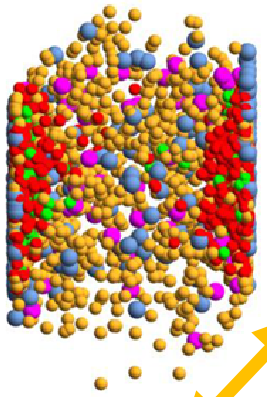

QGP out-of equilibrium ←→ HIC

Parton-Hadron-String-Dynamics (PHSD)

controled by

experimental data

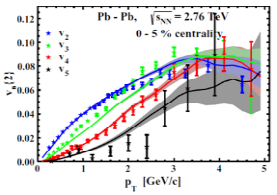

Partonic interactions → DQPM
hadronic interactions → hadron physics
In-medium hadronic interactions → many-body physics: G-matrix

From SIS to LHC: from hadrons to partons

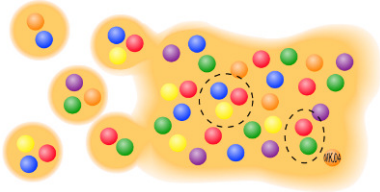

The goal: to study of the phase transition from hadronic to partonic matter and properties of the Quark-Gluon-Plasma on a microscopic level

➔ need a consistent non-equilibrium transport model

- ❑ with explicit parton-parton interactions (i.e. between quarks and gluons)
- ❑ explicit phase transition from hadronic to partonic degrees of freedom
- ❑ lQCD EoS for partonic phase (‚cross over' at μ_q=0)

- ❑ Transport theory for strongly interacting systems: off-shell Kadanoff-Baym equations for the Green-functions $S^{<}_{h}(x,p)$ in phase-space representation for the partonic and hadronic phase

➔ **Parton-Hadron-String-Dynamics (PHSD)**

QGP phase described by

Dynamical QuasiParticle Model (DQPM)

W. Cassing, E. Bratkovskaya, PRC 78 (2008) 034919; NPA831 (2009) 215; W. Cassing, EPJ ST 168 (2009) 3

A. Peshier, W. Cassing, PRL 94 (2005) 172301; Cassing, NPA 791 (2007) 365: NPA 793 (2007)

Dynamical QuasiParticle Model (DQPM) - Basic ideas:

DQPM describes QCD properties in terms of ‚resummed' single-particle Green's functions – in the sense of a two-particle irreducible (2PI) approach:

Gluon propagator: $\Delta^{-1} = P^2 - \Pi$ gluon self-energy: $\Pi = M_g^2 - i2\Gamma_g\omega$

Quark propagator: $S_q^{-1} = P^2 - \Sigma_q$ quark self-energy: $\Sigma_q = M_q^2 - i2\Gamma_q\omega$

- the resummed properties are specified by complex self-energies which depend on temperature:
  - the real part of self-energies (Σ_q, Π) describes a dynamically generated mass (M_q,M_g);
  - the imaginary part describes the interaction width of partons (Γ_q, Γ_g)

- space-like part of energy-momentum tensor $T_{\mu\nu}$ defines the potential energy density and the mean-field potential (1PI) for quarks and gluons (U_q, U_g)

- 2PI framework guaranties a consistent description of the system in- and out-off equilibrium on the basis of Kadanoff-Baym equations with proper states in equilibrium

A. Peshier, W. Cassing, PRL 94 (2005) 172301;
Cassing, NPA 791 (2007) 365: NPA 793 (2007)

The Dynamical QuasiParticle Model (DQPM)

- **Basic idea: interacting quasi-particles: massive quarks and gluons (g, q, q_{bar}) with Lorentzian spectral functions :**

$$\rho_i(\omega,T) = \frac{4\omega\Gamma_i(T)}{\left(\omega^2 - \vec{p}^{\,2} - M_i^{\,2}(T)\right)^2 + 4\omega^2\Gamma_i^2(T)} \qquad (i = q,\bar{q},g)$$

- **fit to lattice (lQCD) results (e.g. entropy density) with 3 parameters**

➔ **Quasi-particle properties:**
large width and mass for gluons and quarks

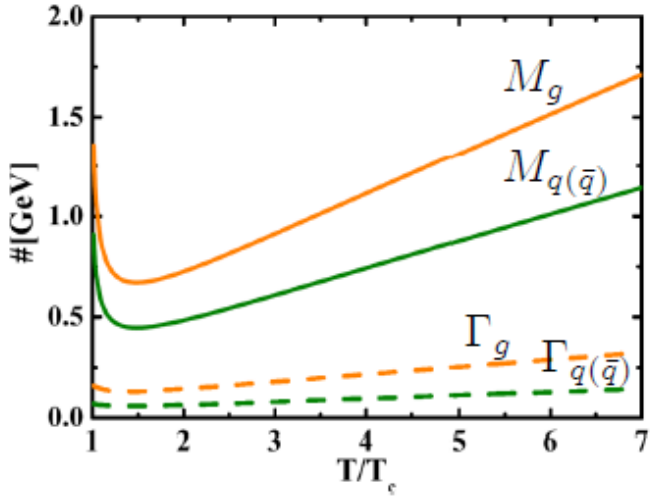

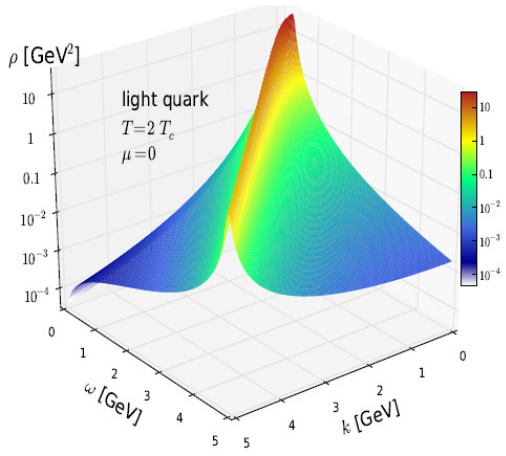

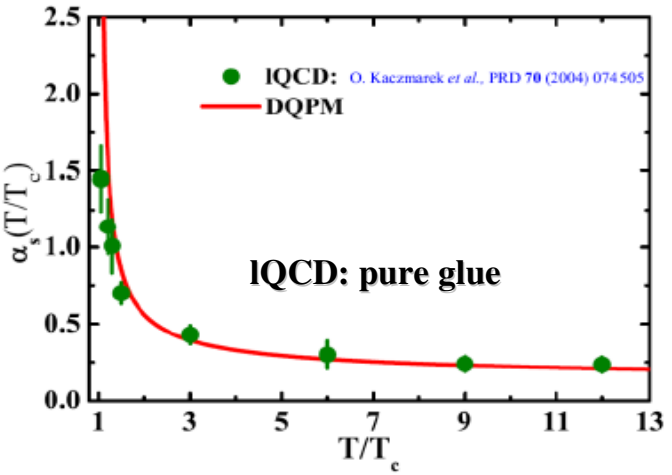

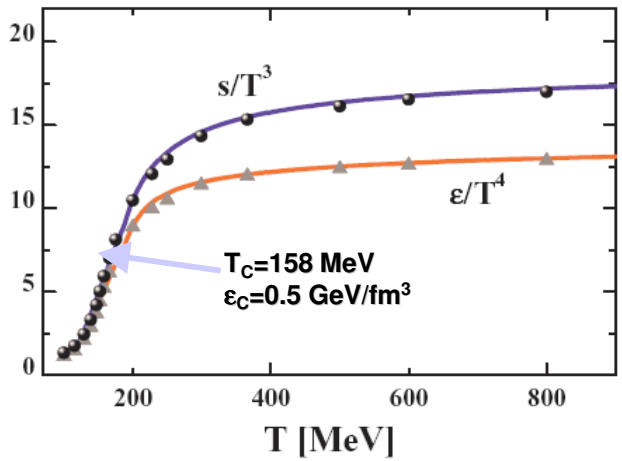

- **DQPM provides mean-fields (1PI) for gluons and quarks as well as effective 2-body interactions (2PI)**
- **DQPM gives transition rates for the formation of hadrons**
  → PHSD

DQPM: Peshier, Cassing, PRL 94 (2005) 172301;
Cassing, NPA 791 (2007) 365: NPA 793 (2007)

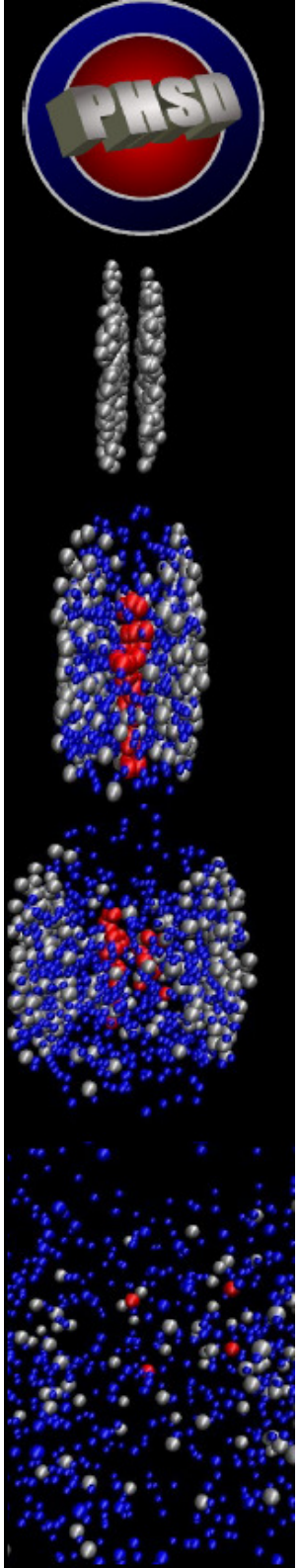

Parton-Hadron-String-Dynamics (PHSD)

- **Initial A+A collisions – HSD:**
  N+N → string formation → decay to pre-hadrons

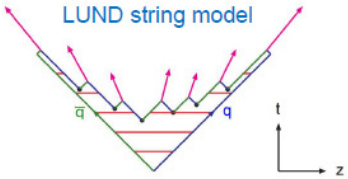

- **Formation of QGP stage if $\varepsilon > \varepsilon_{critical}$:**
  dissolution of pre-hadrons → (DQPM) →
  → massive quarks/gluons + mean-field potential U_q

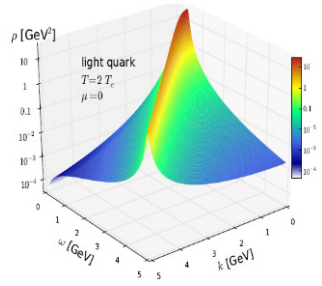

- **Partonic stage – QGP :**
  based on the Dynamical Quasi-Particle Model (DQPM)

  - **(quasi-) elastic collisions:**

$$q+q \to q+q \qquad g+q \to g+q$$
$$q+\bar{q} \to q+\bar{q} \qquad g+\bar{q} \to g+\bar{q}$$
$$\bar{q}+\bar{q} \to \bar{q}+\bar{q} \qquad g+g \to g+g$$

  - **inelastic collisions:**

$$q+\bar{q} \to g \qquad q+\bar{q} \to g+g$$
$$g \to q+\bar{q} \qquad g \to g+g$$

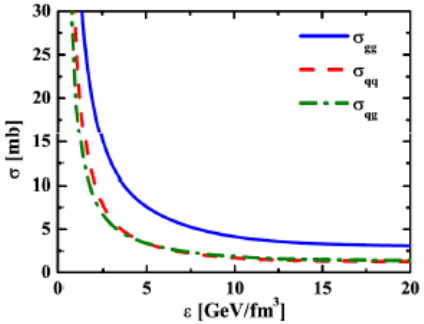

- **Hadronization (based on DQPM):**

$$g \to q+\bar{q}, \qquad q+\bar{q} \leftrightarrow meson \ (or\ 'string')$$
$$q+q+q \leftrightarrow baryon \ (or\ 'string')$$

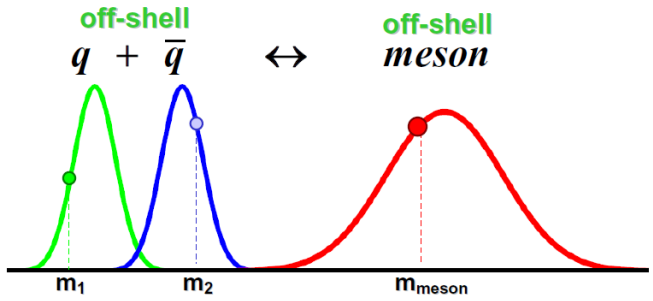

- **Hadronic phase: hadron-hadron interactions – off-shell HSD**

W. Cassing, E. Bratkovskaya, PRC 78 (2008) 034919; NPA831 (2009) 215; W. Cassing, EPJ ST 168 (2009) 3

QGP in equilibrium: Transport properties at finite (T, μ_q): η/s

Infinite hot/dense matter = PHSD in a box:

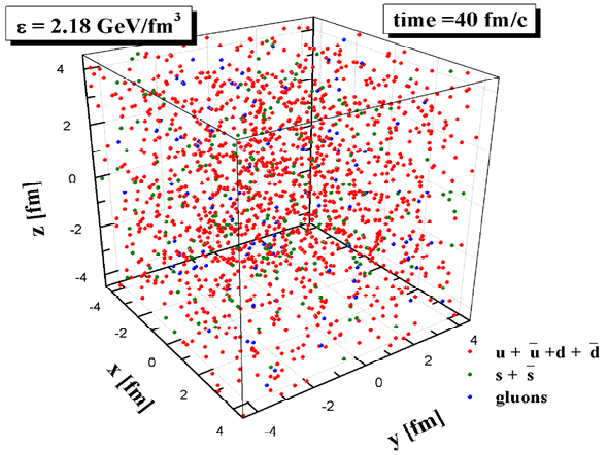

Shear viscosity η/s at finite T

V. Ozvenchuk et al., PRC 87 (2013) 064903

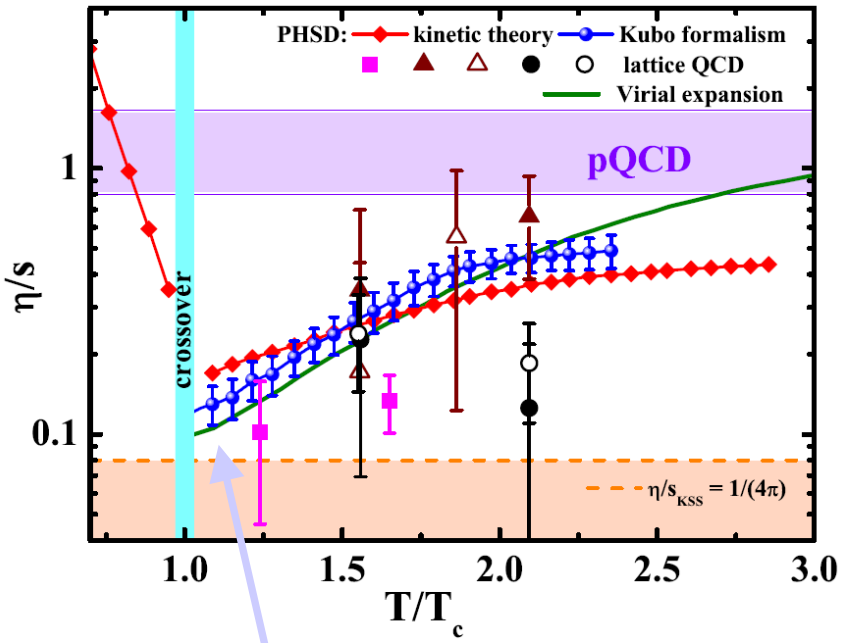

Shear viscosity η/s at finite (T, μ_q)

IQCD:

$$\frac{T_c(\mu_q)}{T_c(\mu_q=0)} = \sqrt{1-\alpha\,\mu_q^2} \approx 1-\alpha/2\,\mu_q^2+\cdots$$

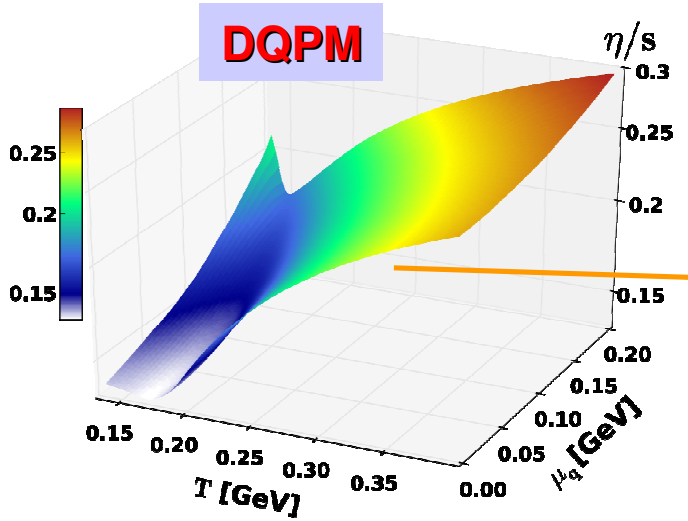

QGP in PHSD = strongly-interacting liquid

η/s: μ_q=0 ➔ finite μ_q: smooth increase as a function of (T, μ_q)

H. Berrehrah et al. arXiv:1412.1017

Non-equilibrium dynamics: description of A+A with PHSD

❑ **Important:** to be conclusive on charm observables, the **light quark dynamics** must be well under control!

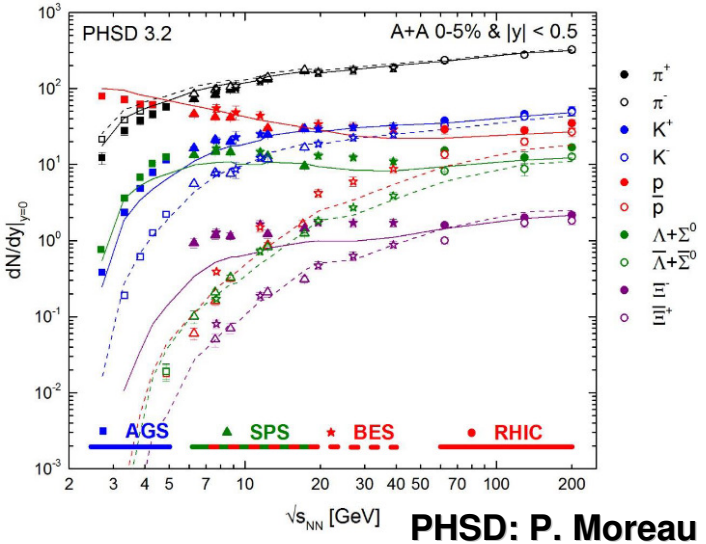

PHSD: P. Moreau

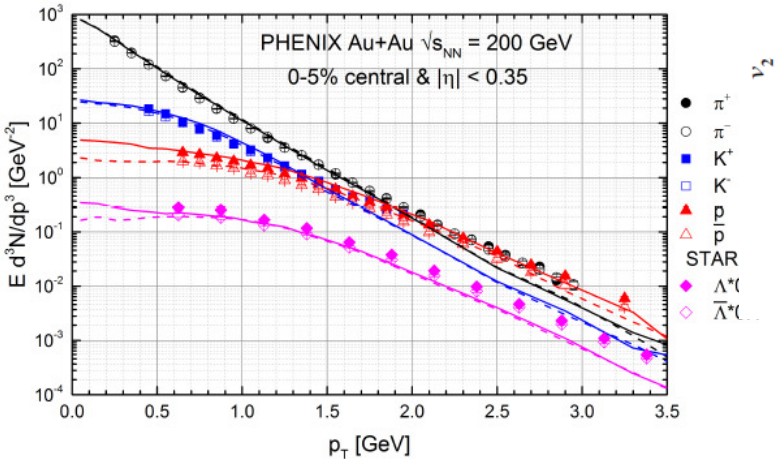

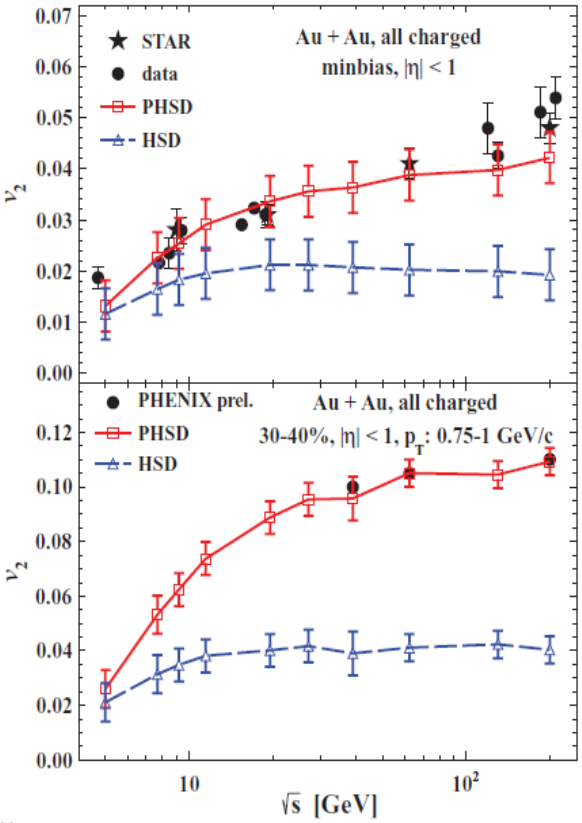

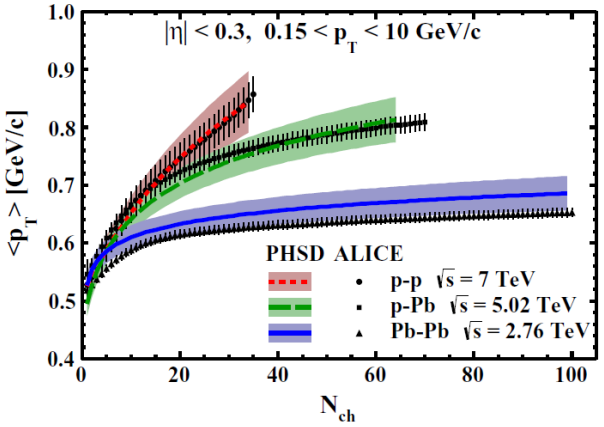

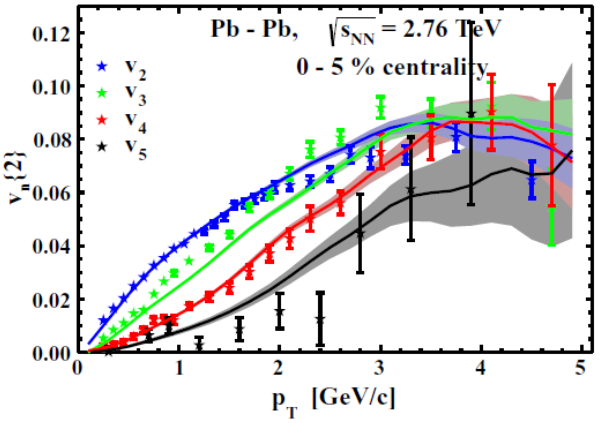

V. Konchakovski et al.,
PRC 85 (2012) 011902; JPG42 (2015) 055106

❑ **PHSD** provides a **good description of ‚bulk' observables** (y-, p_T-distributions, flow coeficients v_n, …) from SPS to LHC

Charm quark production in A+A

- A+A: charm production in initial NN binary collisions: probability $P = \frac{\sigma(c\bar{c})}{\sigma_{NN}^{inel}}$

- The total cross section for charm production in p+p collisions σ(cc)

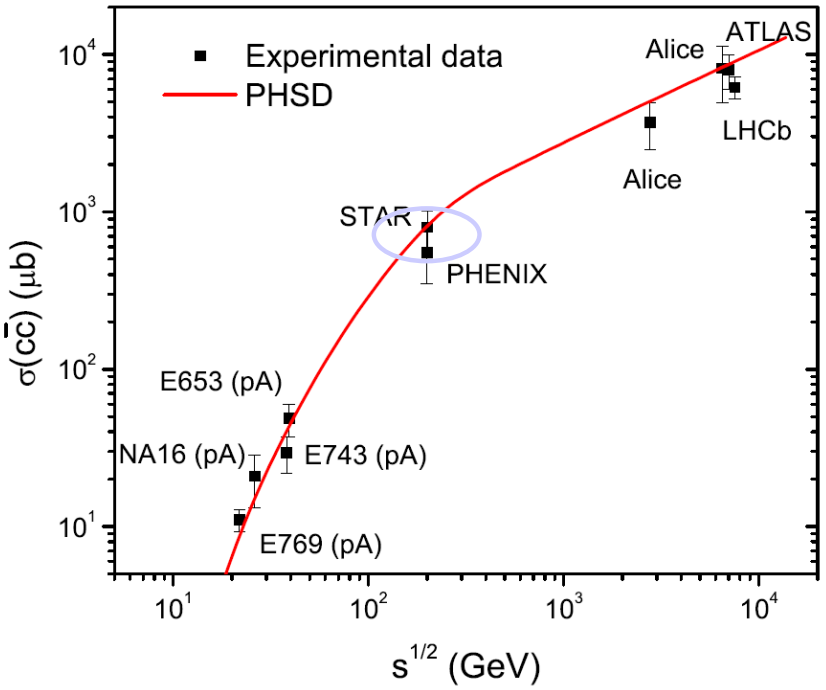

- The energy distribution of binary NN collision including Fermi smearing

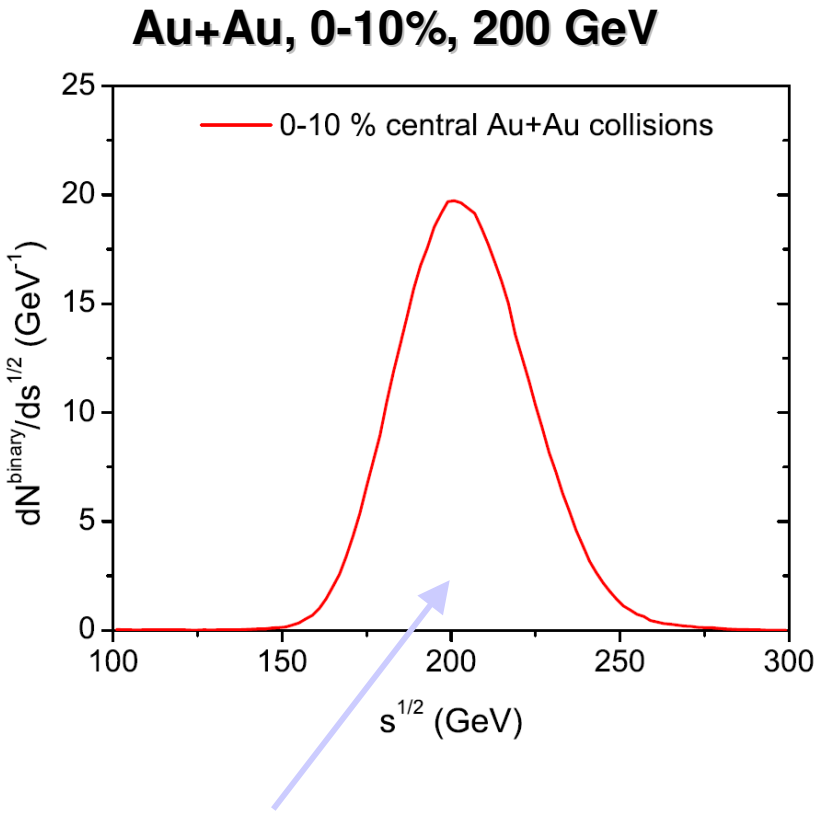

Collision energy smearing due to the Fermi motion

T. Song et al., PRC 92 (2015) 014910, arXiv:1503.03039

Charm quark/hadrons production in p+p collisions

1) Momentum distribution of charm quark: use ‚tuned' PYTHIA event generator to reproduce FONLL (fixed-order next-to-leading log) results (R. Vogt et al.)

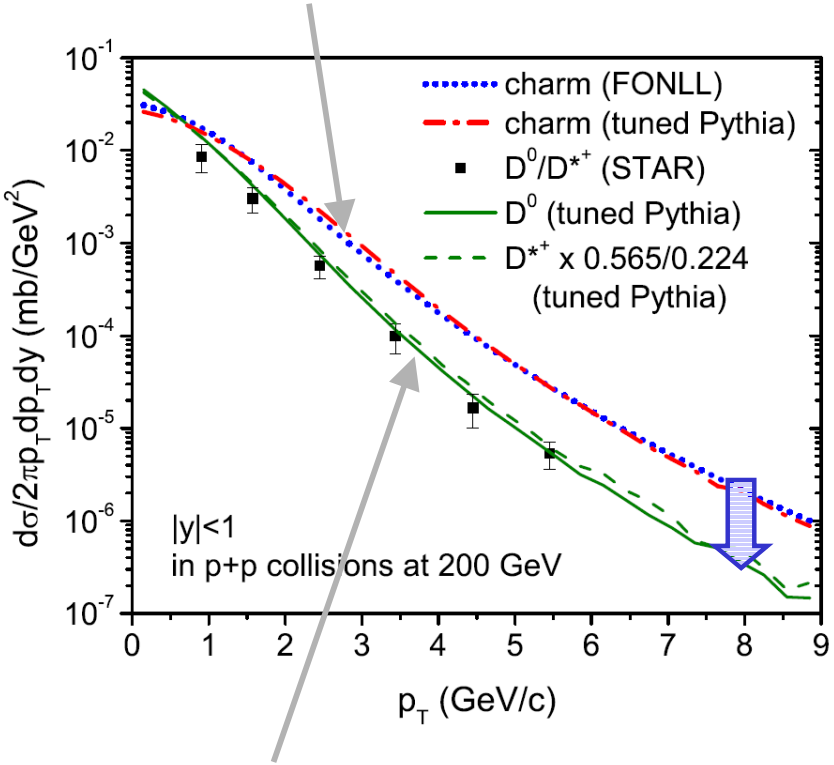

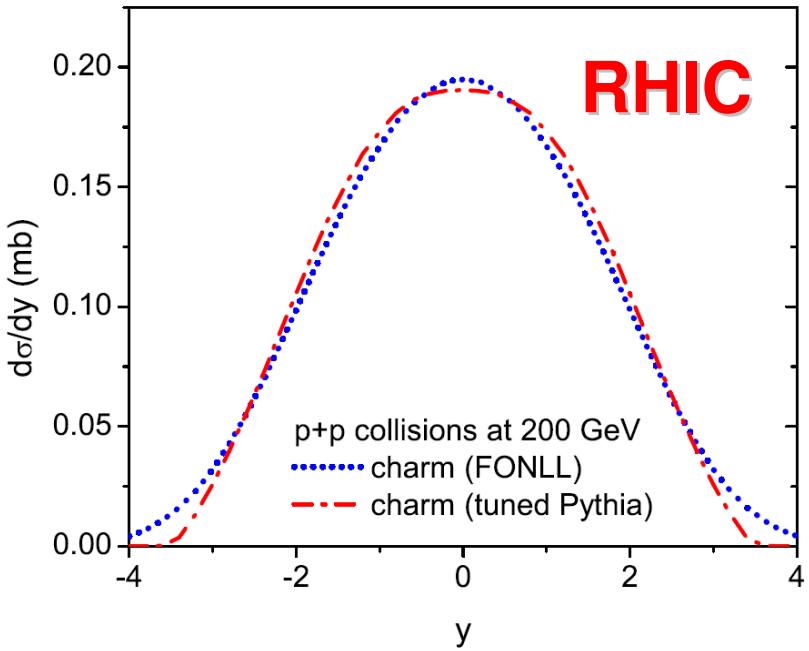

T. Song et al., PRC 92 (2015) 014910, arXiv:1503.03039

2) Charm hadron production by c-quark fragmentation:

D⁰ 20 %
D⁺ 17.4 %
D*⁰ 21.3 %
D*⁺ 22.4 %
Ds⁺ 8 %
Λ_c 9.4 %

$$D_Q^H(z) \sim \frac{1}{z[1-1/z-\epsilon_Q/(1-z)]^2}$$

From C. Peterson et al., PRD27 (1983) 105

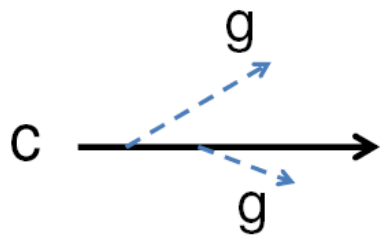

- z : momentum fraction of hadron H in heavy quark Q
- ε_Q=0.01 for Q=charm

Charm quark/hadrons production in p+p collisions

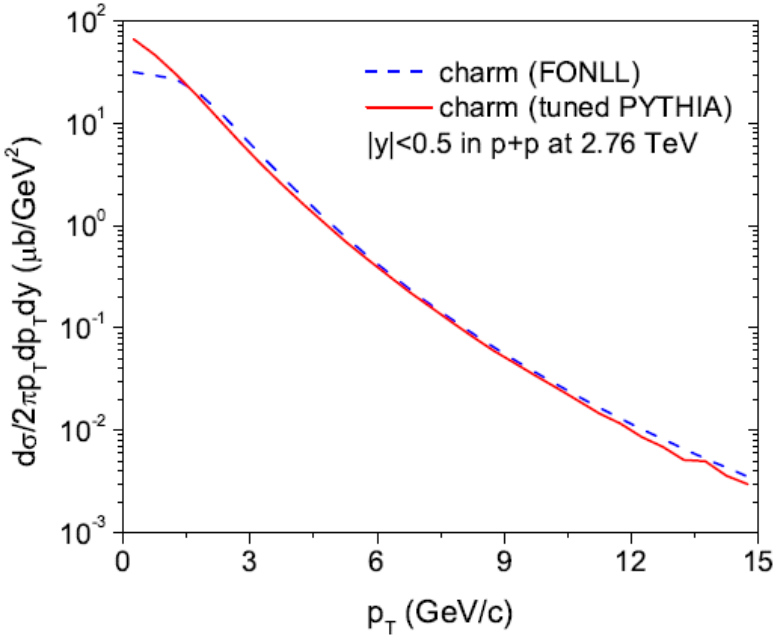

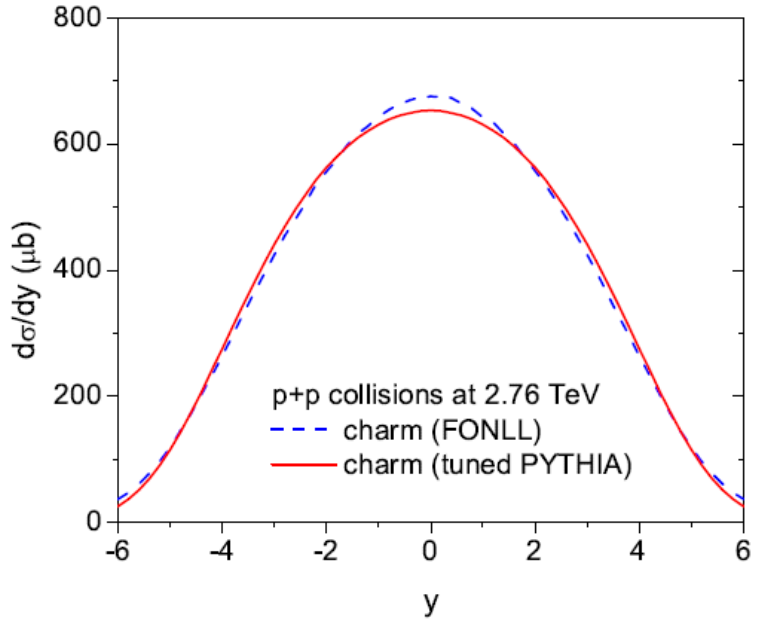

LHC

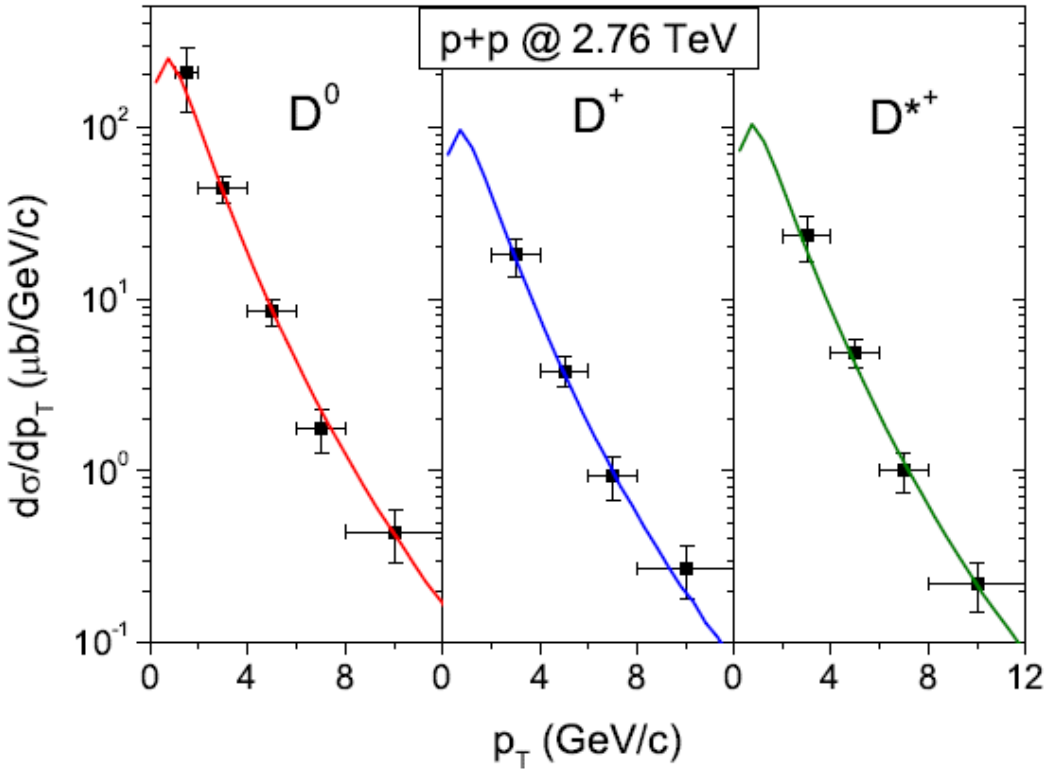

Momentum distribution of charm quark:

use ‚tuned' PYTHIA event generator to reproduce FONLL (fixed-order next-to-leading log) results (R. Vogt et al.)

T. Song et al., arXiv:1512.0089

Charm quark scattering in the QGP (DQPM)

- **Elastic scattering with off-shell massive partons Q+q(g)→Q+q(g)**

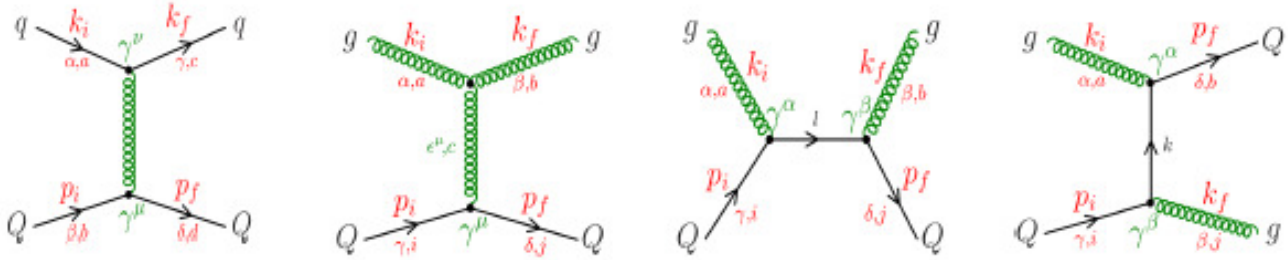

Non-perturbative QGP!

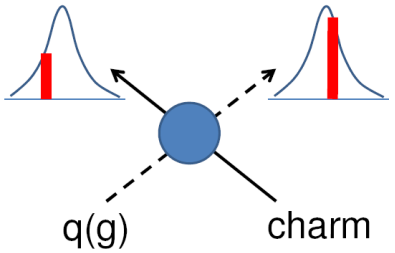

- **Elastic cross section uc→uc**

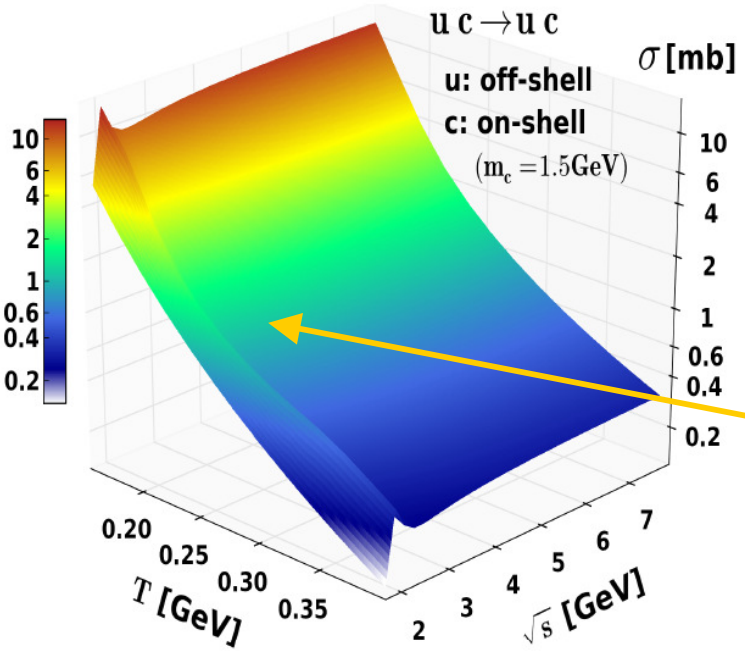

- **Distributions of Q+q, Q+g collisions vs $s^{1/2}$ in Au+Au, 10% central**

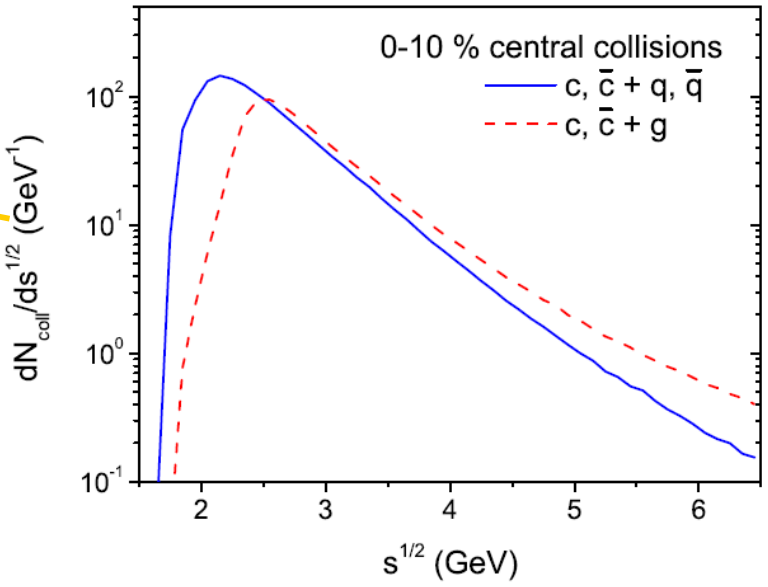

H. Berrehrah et al, PRC 89 (2014) 054901;
PRC 90 (2014) 051901; PRC90 (2014) 064906

Charm quark scattering in the QGP

❑ **Differential elastic cross section** for uc→uc for $s^{1/2}$=3 and 4 GeV at $1.2T_C$, $2T_C$ and $3T_C$

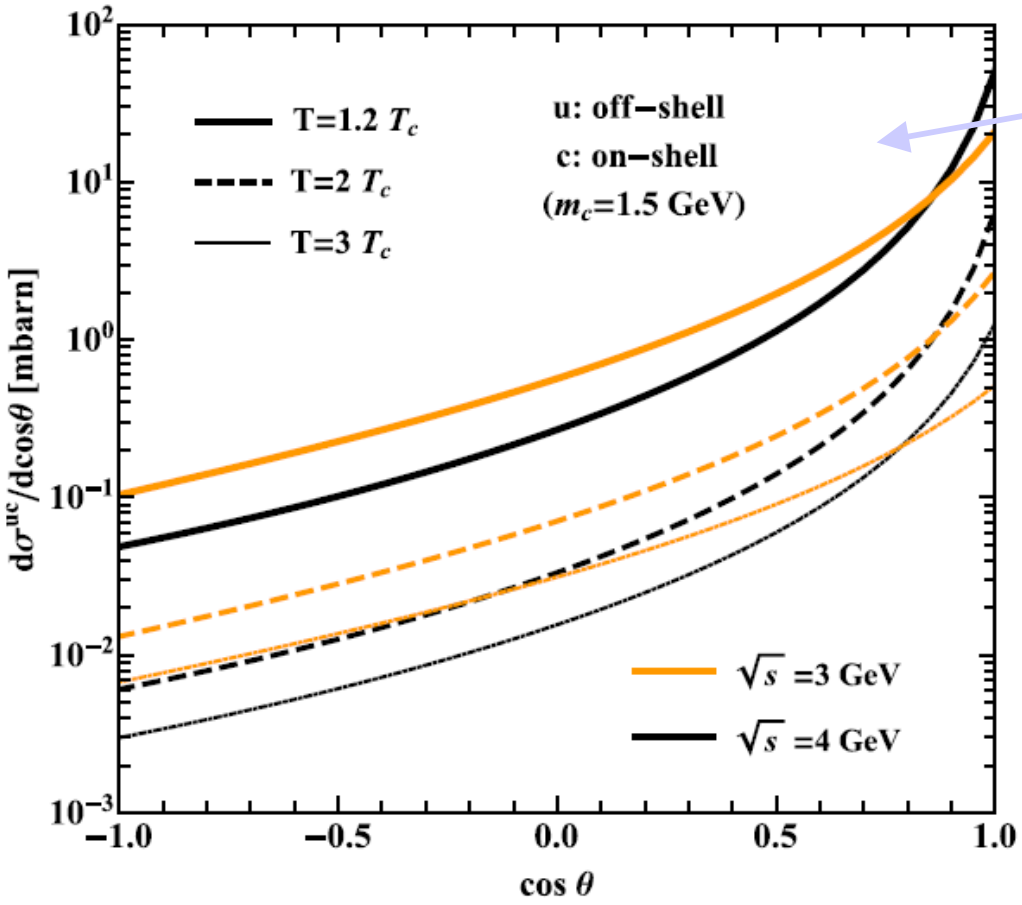

❑ **DQPM - anisotropic angular distribution**

Note: pQCD - strongly forward peaked
➔ **Differences between DQPM and pQCD** :
less forward peaked angular distribution
leads to **more efficient momentum transfer**

❑ N(cc) ~19 pairs,
N(Q+q)~130, N(Q+g) ~85 collisions
➔ each charm quark makes
~ 6 elastic collisions

➔ **Smaller number** (compared to **pQCD**)
of elastic scatterings with massive
partons leads to a **large energy loss**

! **Note**: **radiative energy loss** is **NOT included** yet in PHSD (work in progress);
expected to be **small** due to the large gluon mass in the DQPM

H. Berrehrah et al, PRC 89 (2014) 054901; PRC 90 (2014) 051901; PRC90 (2014) 064906

Charm spatial diffusion coefficient D_s in the hot medium

- **D_s for heavy quarks as a function of T for μ_q=0 and finite μ_q assuming adiabatic trajectories (constant entropy per net baryon s/n_B) for the expansion**

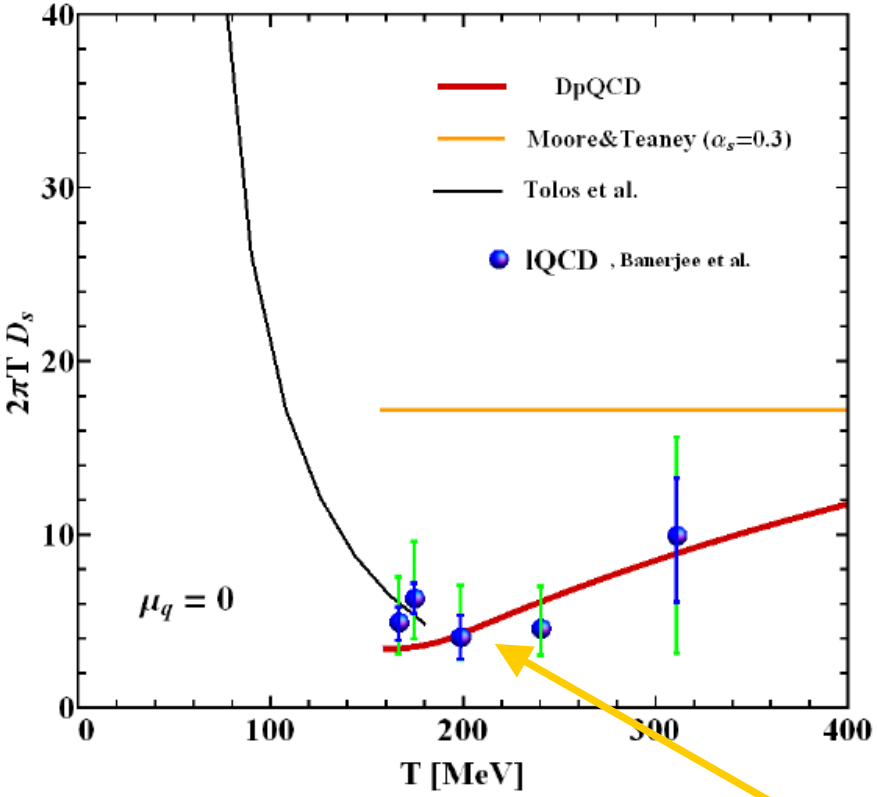

$\Rightarrow$ $\mu_q \neq 0$

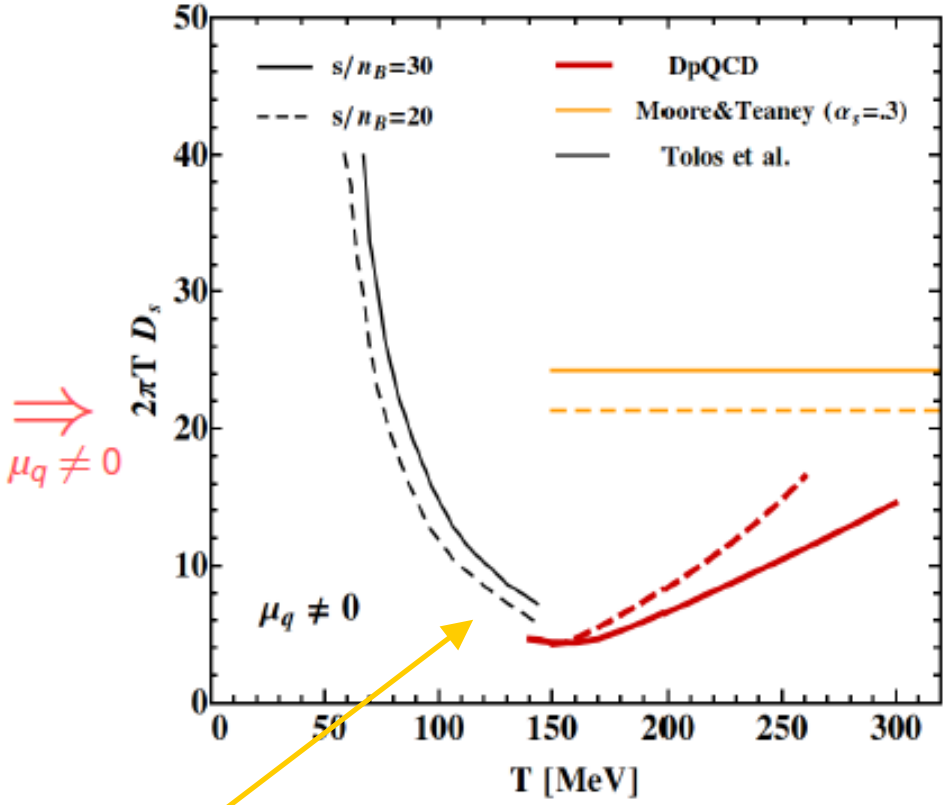

➔ **Continuous transition at T_C!**

❑ **$T < T_c$: hadronic D_s**

L. Tolos , J. M. Torres-Rincon, PRD 88 (2013) 074019
V. Ozvenchuk et al., PRC90 (2014) 054909

H. Berrehrah et al, PRC 90 (2014) 051901, arXiv:1406.5322

Thermalization of charm quarks in A+A ?

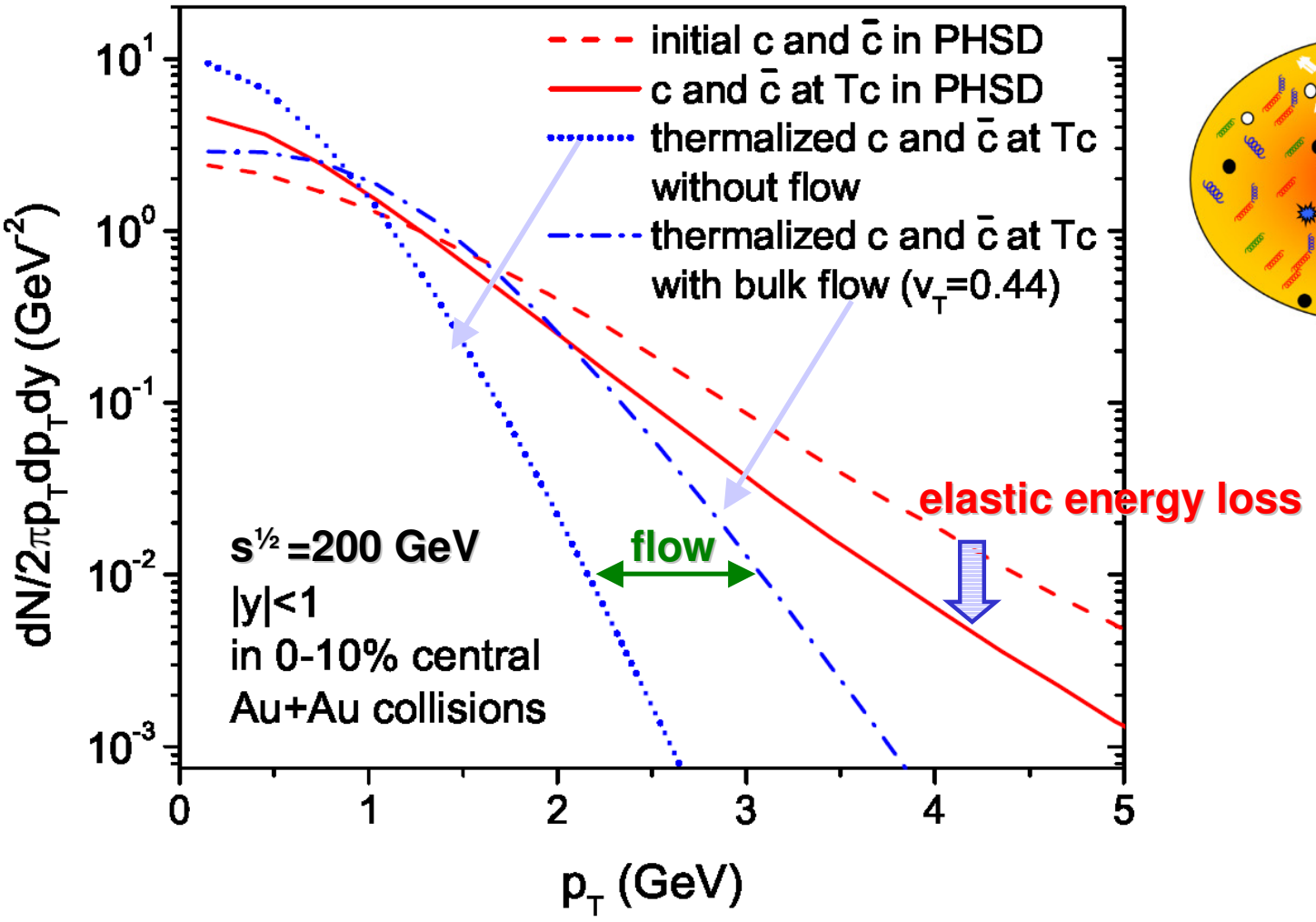

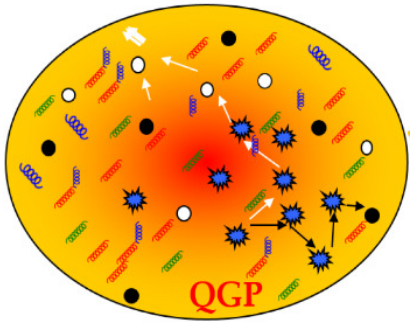

- Scattering of charm quarks with massive partons softens the p_T spectra
  ➔ elastic energy loss
- Charm quarks are close to thermal equilibrium at low $p_T < 2$ GeV/c

T. Song et al., PRC 92 (2015) 014910, arXiv:1503.03039

Hadronization of charm quarks in A+A

❑ **PHSD: if the local energy density $\varepsilon < \varepsilon_C$ ➔ hadronization of charm quarks to hadrons:**

1. Dynamical coalescence model

ε_C =0.5 GeV/fm^3

Probability for charm quark/antiquark and the light quark/antiquark to form a meson:

$$f(\boldsymbol{\rho}, \mathbf{k}_\rho) = \frac{8 g_M}{6^2} \exp\left[-\frac{\boldsymbol{\rho}^2}{\delta^2} - \mathbf{k}_\rho^2 \delta^2\right]$$

Degeneracy factor:
g_M = 1 for D
g_M = 3 for D*

D*:
$D^*_0(2400)^0$
$D^*_1(2420)^0$
$D^*_2(2460)^{0\pm}$

where $\boldsymbol{\rho} = \frac{1}{\sqrt{2}}(\mathbf{r}_1 - \mathbf{r}_2), \quad \mathbf{k}_\rho = \sqrt{2}\,\frac{m_2 \mathbf{k}_1 - m_1 \mathbf{k}_2}{m_1 + m_2}$

Width δ ← from root-mean-square radius of meson:

$$\langle r^2 \rangle = \frac{3}{2}\frac{m_1^2 + m_2^2}{(m_1 + m_2)^2}\delta^2$$

Hadronization scenarios :

1: only fragmentation
2. coalescence with <r>=0.5 fm + fragmentation
3: coalescence with <r>=0.9 fm + fragmentation

2. Fragmentation (as in pp)
- if NOT hadronized by coalescence

Note: large <r> used also in Refs:
S. Cao, G. Y. Qin and S. A. Bass, PRC 88, 044907 (2013).
Y. Oh, C. M. Ko, S. H. Lee and S. Yasui, PRC 79, 044905 (2009)

Hadronization of charm quarks in A+A : RHIC

Hadronization scenarios :

1: only fragmentation
2: coalescence with <r>=0.5 fm + fragmentation
3: coalescence with <r>=0.9 fm + fragmentation

$\varepsilon < 0.5$ GeV/fm^3

Coalescence probability in Au+Au

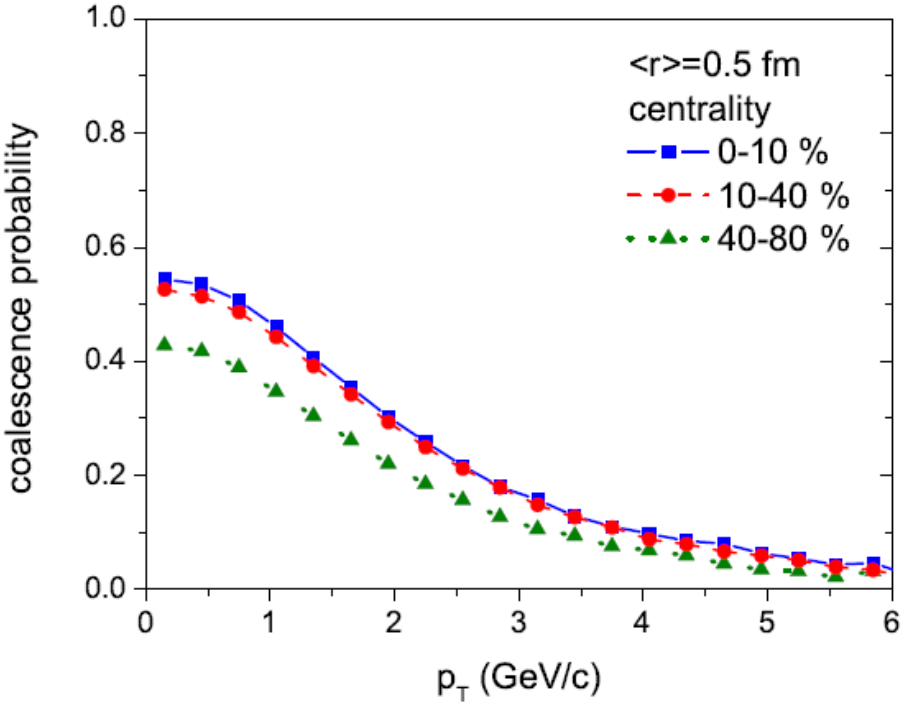

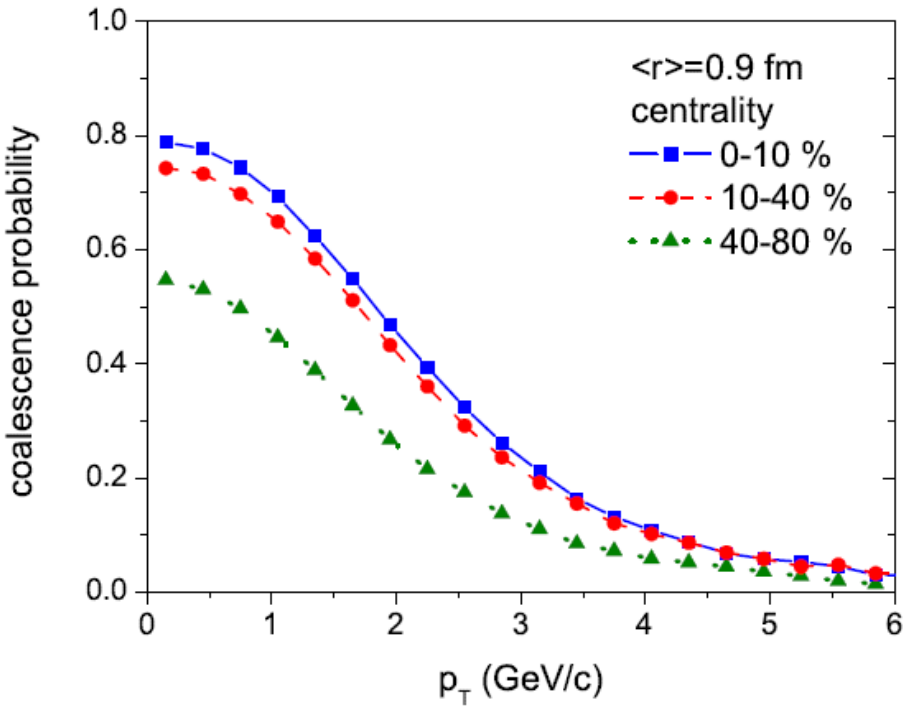

T. Song et al., PRC 92 (2015) 014910, arXiv:1503.03039

Hadronization of charm quarks in A+A : LHC

Dynamical Hadronization scenarios :

4. coalescence with <r>=0.9 fm... + fragmentation

$0.4 < \varepsilon < 0.75$ GeV/fm^3 $\varepsilon < 0.4$ GeV/fm^3

Coalescence probability in Au+Au

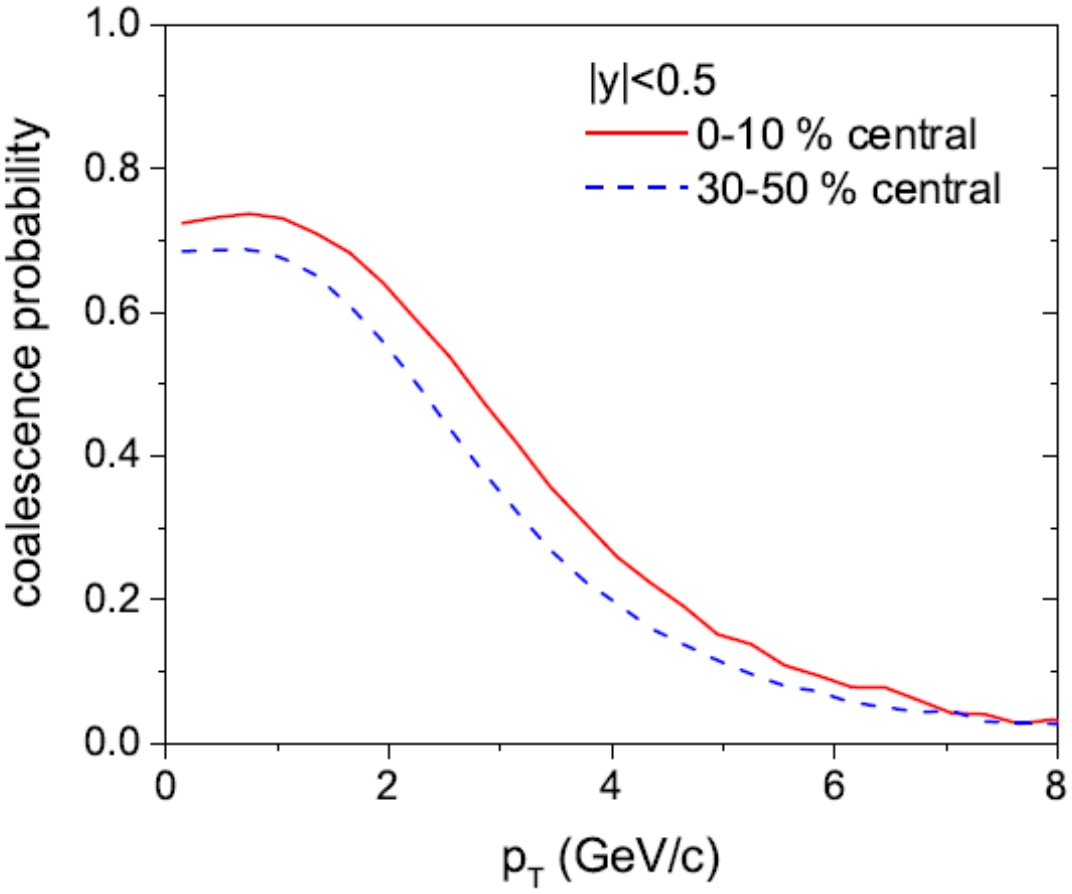

T. Song et al., arXiv:1512.0089

Modelling of D-meson scattering in the hadronic gas

1. D-meson scattering with mesons

Model: effective chiral Lagrangian approach with heavy-quark spin symmetry

L. M. Abreu, D. Cabrera, F. J. Llanes-Estrada, J. M. Torres-Rincon, Annals Phys. 326, 2737 (2011)

Interaction of D=(D^0,D^+,D^+_s) and D*=(D^{*0},D^{*+},D^{*+}_s) with octet (π,K,Kbar,η) :

$$\begin{aligned}\mathcal{L}_{LO} &= \langle\nabla^\mu D\nabla_\mu D^\dagger\rangle - m_D^2\langle DD^\dagger\rangle - \langle\nabla^\mu D^{*\nu}\nabla_\mu D^{*\dagger}_\nu\rangle \\ &+ m_D^2\langle D^{*\mu}D^{*\dagger}_\mu\rangle + ig\langle D^{*\mu}u_\mu D^\dagger - Du^\mu D^{*\dagger}_\mu\rangle \\ &+ \frac{g}{2m_D}\langle D^*_\mu u_\alpha\nabla_\beta D^{*\dagger}_\nu - \nabla_\beta D^*_\mu u_\alpha D^{*\dagger}_\nu\rangle\epsilon^{\mu\nu\alpha\beta}\end{aligned}$$

with

$$u_\mu = i\left(u^\dagger\partial_\mu u - u\partial_\mu u^\dagger\right)$$

$$U = u^2 = \exp\left(\frac{\sqrt{2}i\Phi}{f}\right) \qquad \Phi = \begin{pmatrix} \frac{1}{\sqrt{2}}\pi^0 + \frac{1}{\sqrt{6}}\eta & \pi^+ & K^+ \\ \pi^- & -\frac{1}{\sqrt{2}}\pi^0 + \frac{1}{\sqrt{6}}\eta & K^0 \\ K^- & \bar{K}^0 & -\frac{2}{\sqrt{6}}\eta \end{pmatrix}$$

2. D-meson scattering with baryons

Model: G-matrix approach: interactions of D=(D^0,D^+,D^+_s) and D*=(D^{*0},D^{*+},D^{*+}_s) with nucleon octet $J^P=1/2^+$ and Delta decuplet $J^P=3/2^+$

C. Garcia-Recio, J. Nieves, O. Romanets, L. L. Salcedo, L. Tolos, Phys. Rev. D 87, 074034 (2013)

Unitarized scattering amplitude ➔ from solution of coupled-channel Bethe-Salpeter equations:

$$T = T + VGT$$

T. Song et al., PRC 92 (2015) 014910, arXiv:1503.03039

D-meson scattering in the hadron gas

1. D-meson scattering with mesons

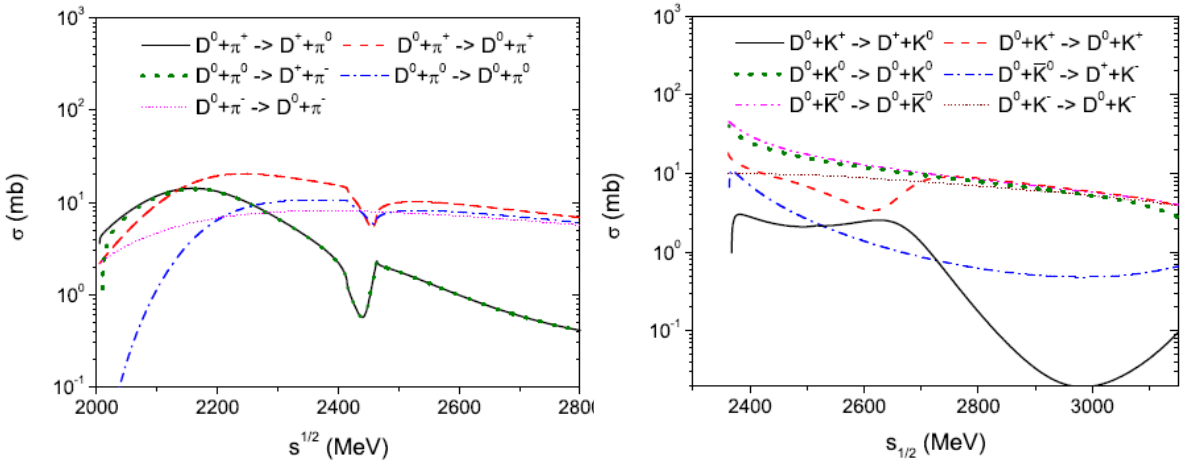

1a) cross sections with $m=\rho,\omega,\phi,K*,...$ taken as

$$\sigma(D, D^* + m) = 10\,mb$$

Distribution $dN/ds^{1/2}$

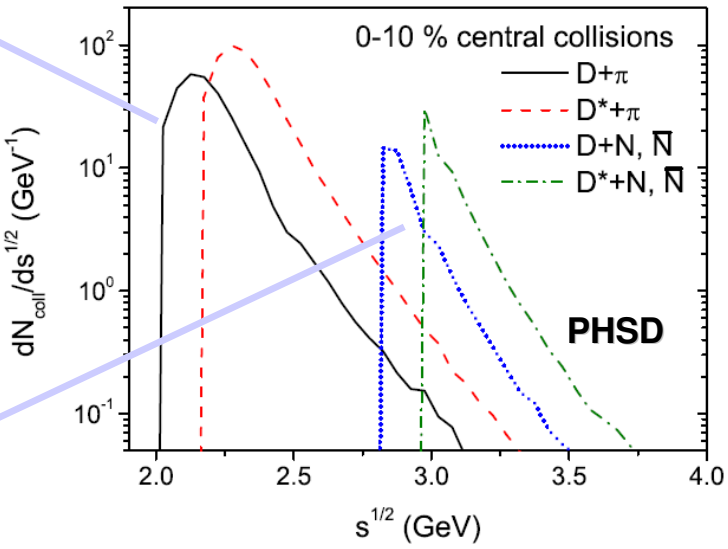

2. D-meson scattering with baryons

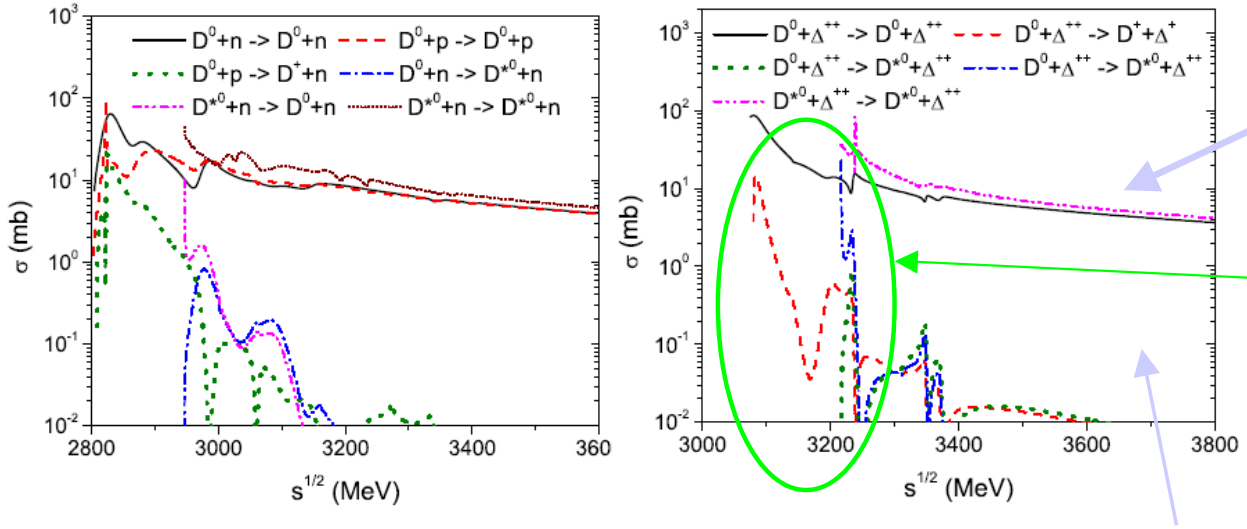

➔**Strong isospin dependence and complicated structure (due to the resonance coupling) of D+m, D+B cross sections!**

➔ **Hadronic interactions become ineffective for the energy loss of D,D* mesons at high transverse momentum (i.e. large $s^{1/2}$)**

R_{AA} at RHIC - coalescence vs fragmentation

1. Influence of hadronization scenarios: coalescence vs fragmentation

! Model study: without any rescattering (partonic and hadronic)

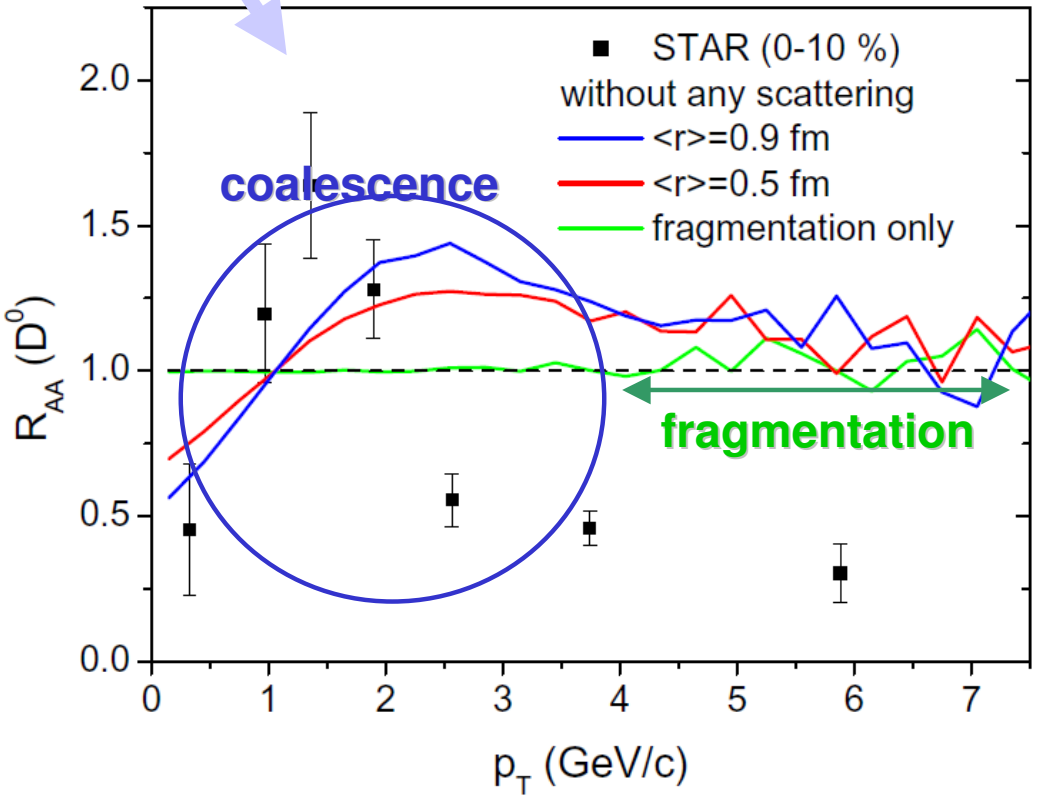

$$R_{AA}(p_T) \equiv \frac{dN_D^{\mathrm{Au+Au}}/dp_T}{N_{\mathrm{binary}}^{\mathrm{Au+Au}} \times dN_D^{\mathrm{p+p}}/dp_T}$$

Coalescence probability in Au+Au

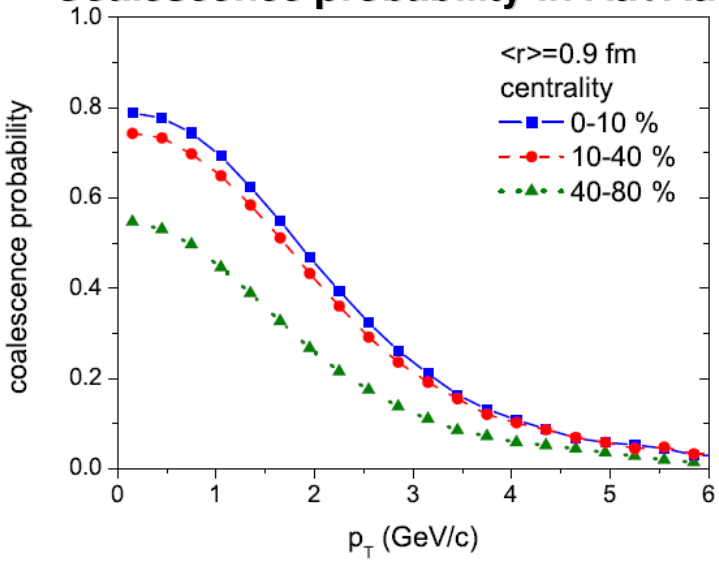

- Expect: no scattering: $R_{AA}=1$
- Hadronization by fragmentation only (as in pp) → $R_{AA}=1$
- Coalescence (not in pp!) shifts R_{AA} to larger p_T ➔ ‚nuclear matter' effect
- The hight of the R_{AA} peak depends on the balance: coalescence vs. fragmentation

R_{AA} at RHIC: partonic scattering

2. Influence of partonic rescattering

! **Model study:** by scaling of parton cross sections: $\sigma(Q+q(g))^*\alpha$ by α=0, 0.5, 1, 2 (without hadronic rescattering)

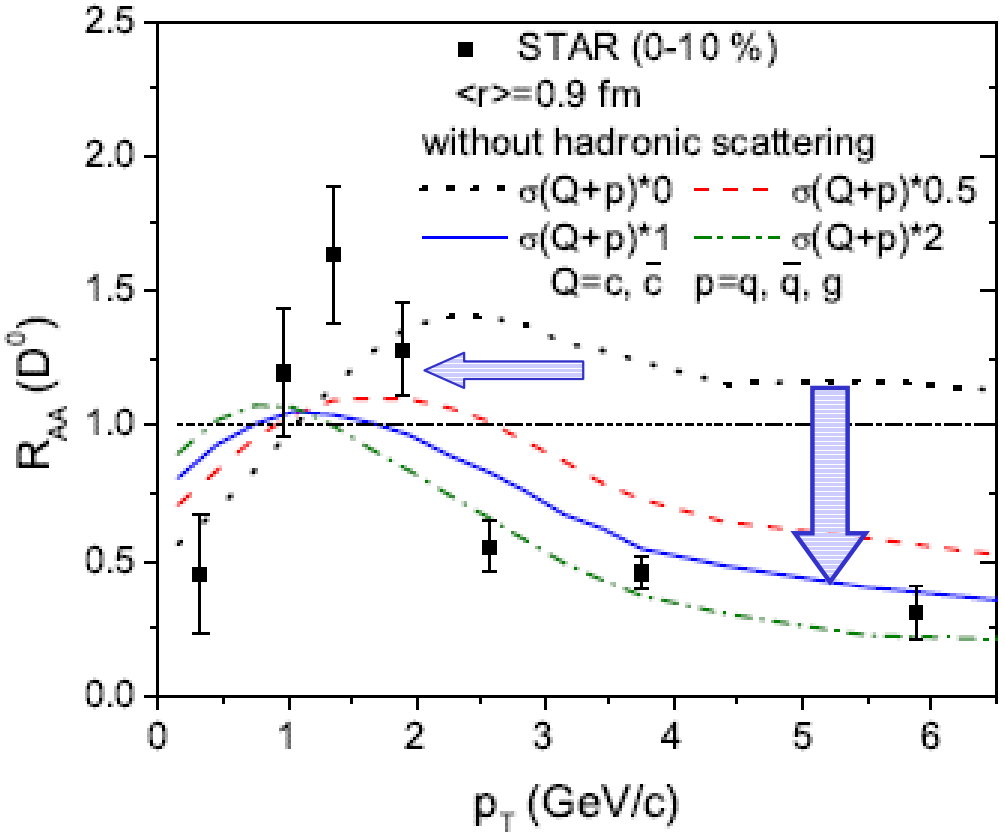

Elliptic flow $v_2(p_T)$

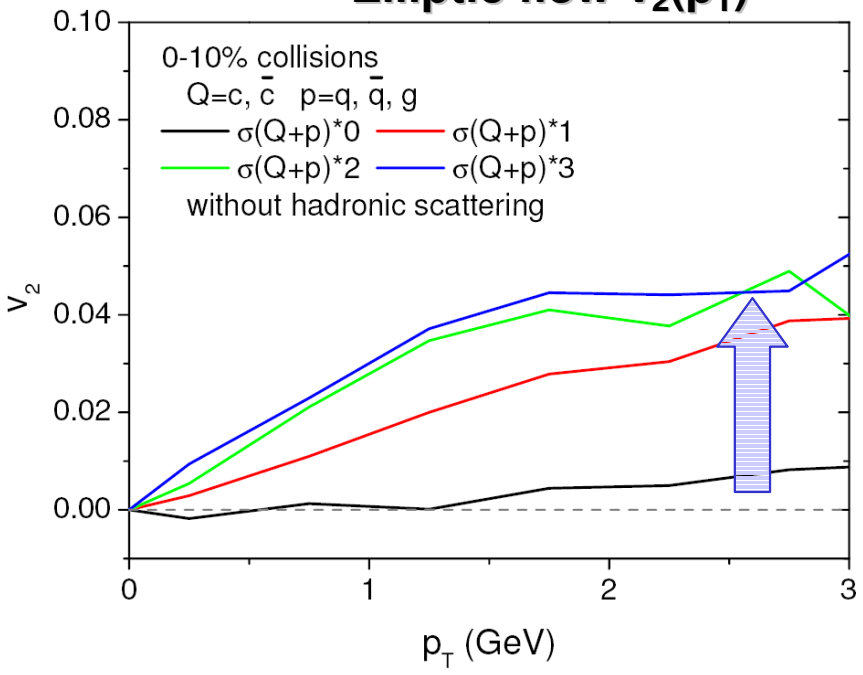

Central Au+Au at $s^{1/2}$ =200 GeV :
N(cc) ~19 pairs,
N(Q+q)~130 collisions
N(Q+g) ~85 collisions

Elastic partonic rescattering
- **moves R_{AA} to lower p_T and suppresses large p_T**
- **increases v_2**

➔ **each charm quark makes ~ 6 elastic collisions**

R_{AA} at RHIC: hadronic rescattering

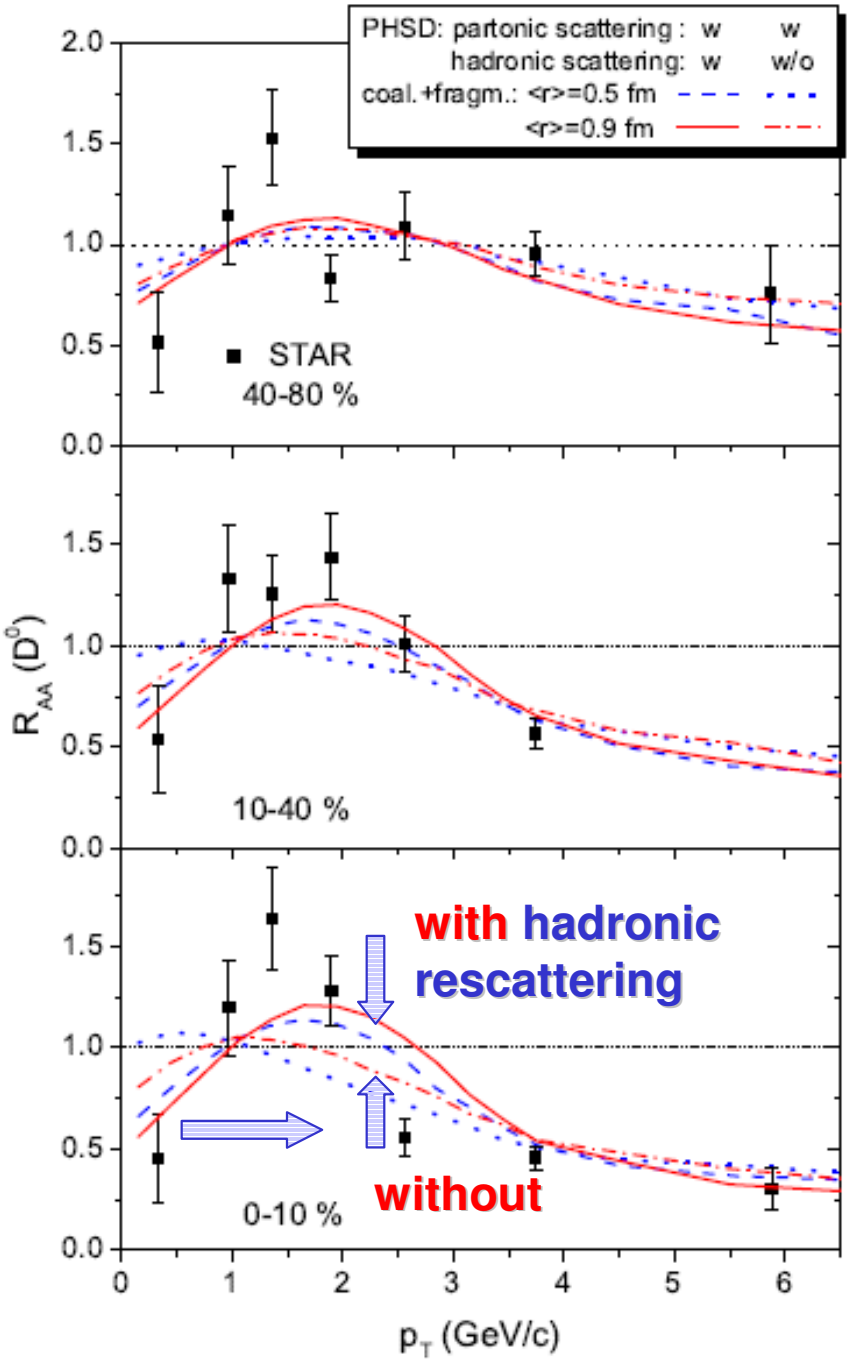

3. Influence of hadronic rescattering

! Model study: (with partonic rescattering)
with / without hadronic rescattering

Central Au+Au at $s^{1/2}$ =200 GeV :
N(D,D*) ~30
N(D,D*+m) ~56 collisions
N(D,D*+B,Bbar) ~10 collisions

➔ **each D,D* makes**
~ 2 scatterings with hadrons

❑ **Hadronic rescattering moves R_{AA} peak to higher p_T !**

T. Song et al., PRC (2015), arXiv:1503.03039
T. Song et al., PRC 92 (2015) 014910, arXiv:1503.03039

D-meson elliptic flow v_2 at RHIC

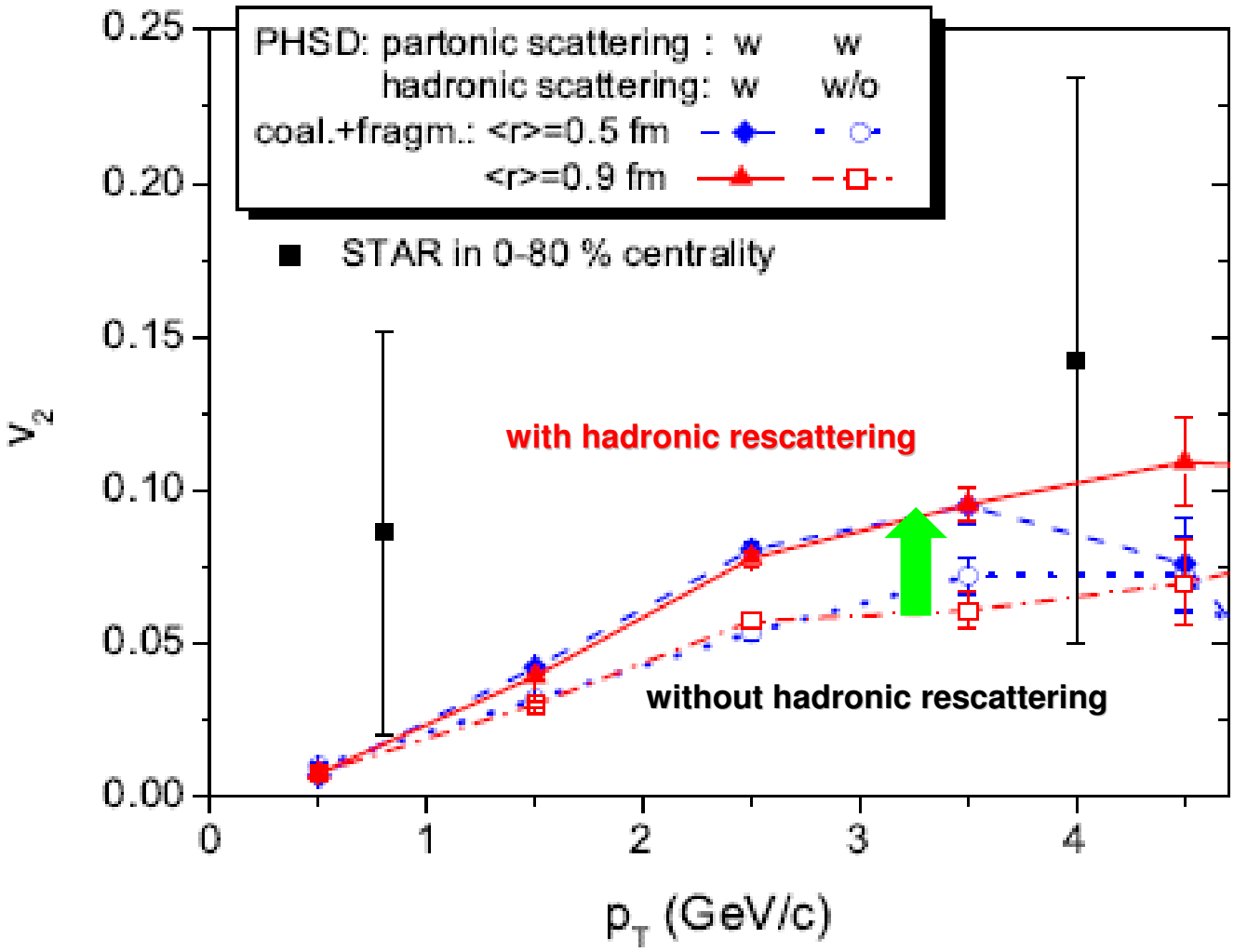

- **Hadronic rescattering substantially increases v_2 at larger p_T**
- **v_2 is less sensitive to the hadronization scenarios than R_{AA}**

T. Song et al., PRC 92 (2015) 014910, arXiv:1503.03039

R_{AA} at RHIC

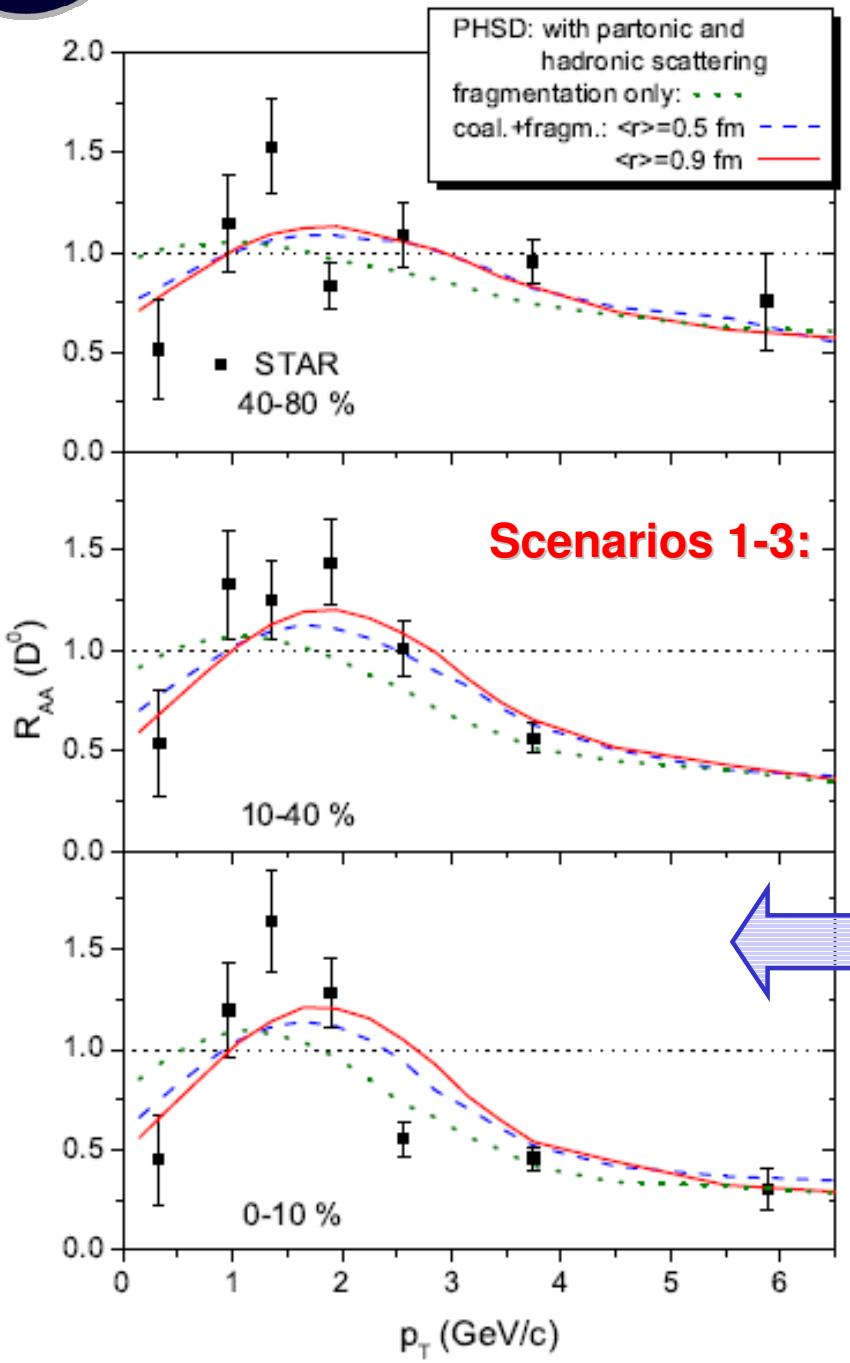

PHSD results:
with all rescattering (partonic and hadronic)

4: Dynamical Hadronization scenario (new)

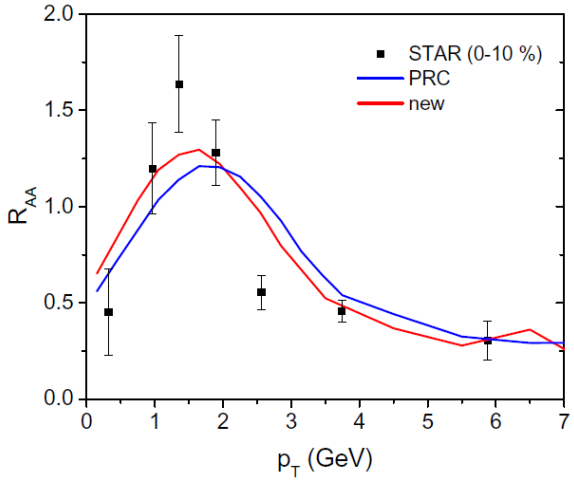

❑ **The hight and position of the R_{AA} peak at low p_T depends on the hadronization scenario: coalescence/fragmentation!**

➔**PHSD: the STAR data are better described within scenario „coalescence with <r>=0.9 fm + fragmentation“ and dynamical hadronization scenario**

T. Song et al., PRC 92 (2015) 014910, arXiv:1503.03039

Shadowing effect

Charm production cross section in N*N* in HIC:

$$\sigma_{c\bar{c}}^{N^*N^*}(s) = \sum_{i,j} \int dx_1 dx_2 R_i^A(x_1,Q) R_j^A(x_2,Q) \times f_i^N(x_1,Q) f_j^N(x_2,Q) \sigma_{c\bar{c}}^{ij}(x_1 x_2 s, Q).$$

$$\sigma_{c\bar{c}}^{N^*N^*}(s) = \langle R_g^{Pb}(x_1,Q) R_g^{Pb}(x_2,Q) \rangle \; \sigma_{c\bar{c}}^{NN}(s)$$

$$x_1 = \frac{M_T}{E_{\rm cm}} e^{y},$$

$$x_2 = \frac{M_T}{E_{\rm cm}} e^{-y},$$

Scale Q = $(M_T^1+M_T^2)/2$

$R_i^A(x_1,Q)$, $R_i^A(x_2,Q)$ for *i=j=gluon* are obtained from the EPS09 using that charm production is dominated by gluon fusion:

$$\sigma(g+g \to c+\bar{c}) / \sigma(q+\bar{q} \to c+\bar{c})$$

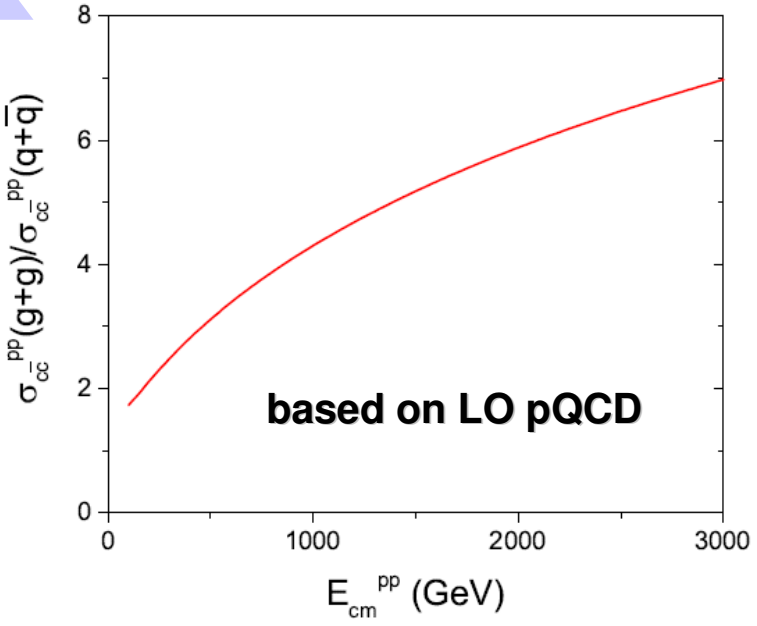

- **The (anti-)shadowing effect depends on the impact parameter in HIC:**

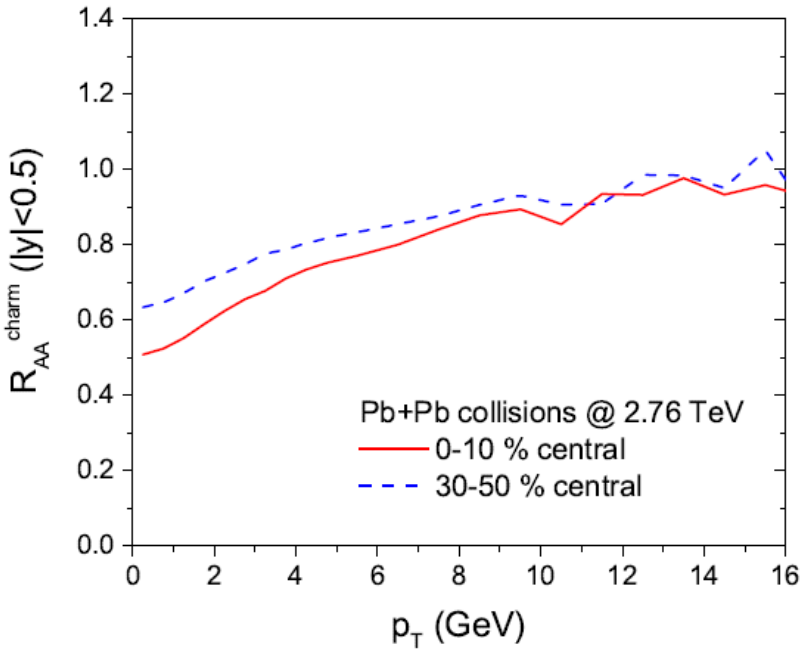

T. Song et al., arXiv:1512.0089

Charm R_{AA} at LHC

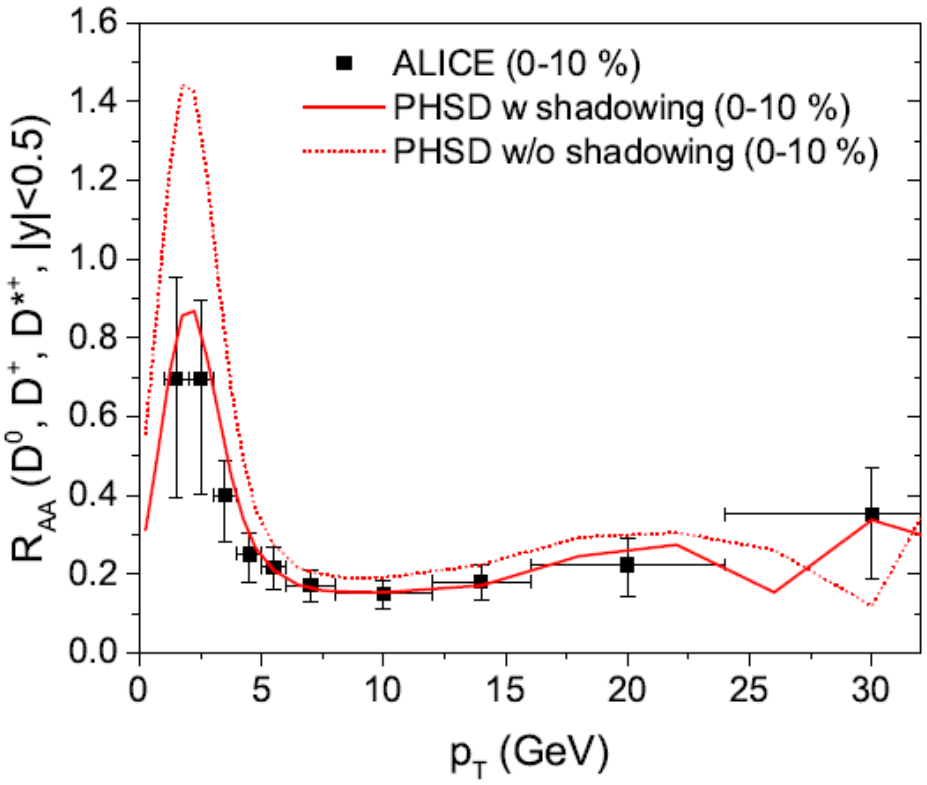

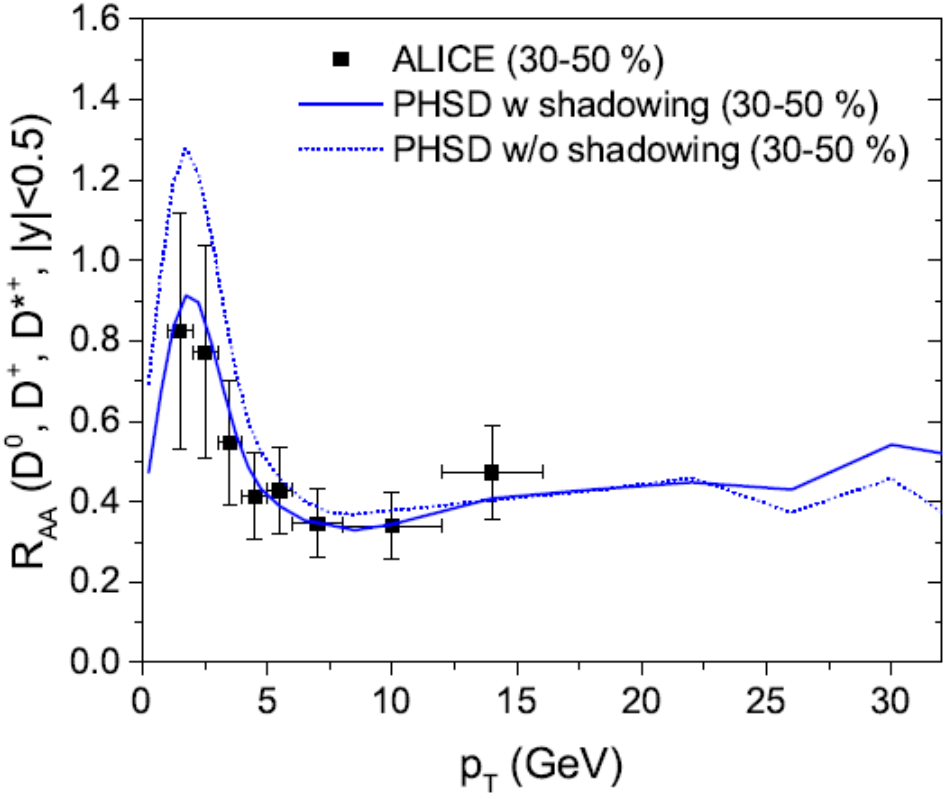

- in PHSD the energy loss of D-mesons at high p_T can be dominantly attributed to partonic scattering
- Shadowing effect suppresses the low p_T and slightly enhanses the high p_T part of R_{AA}
- Hadronic rescattering moves R_{AA} peak to higher p_T

T. Song et al., arXiv:1512.0089

Charm v_2 at LHC

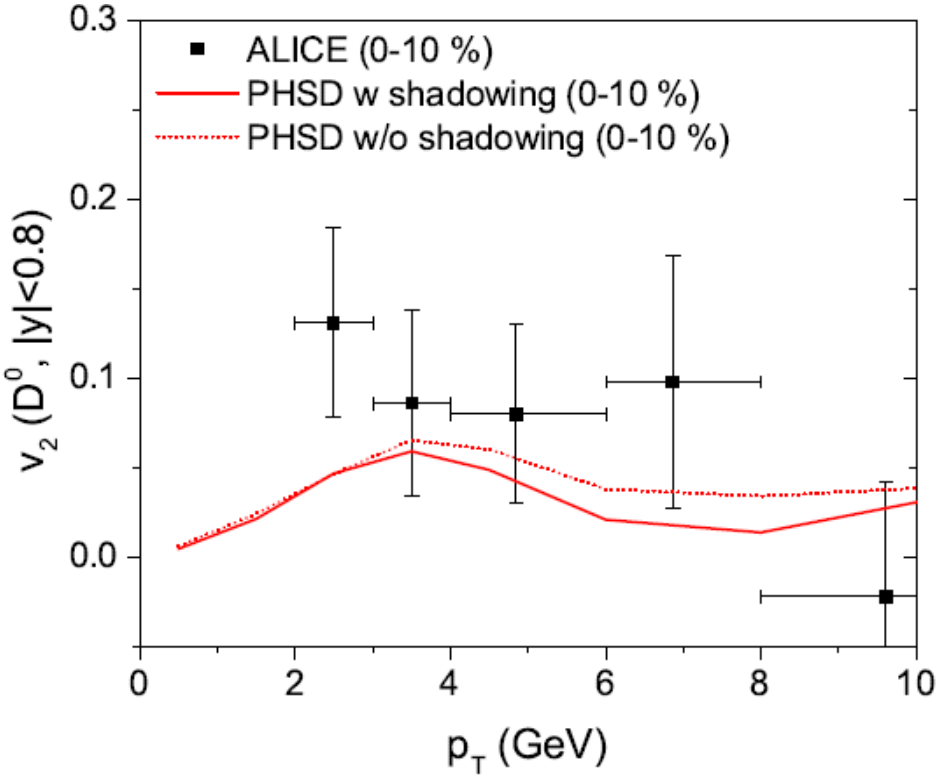

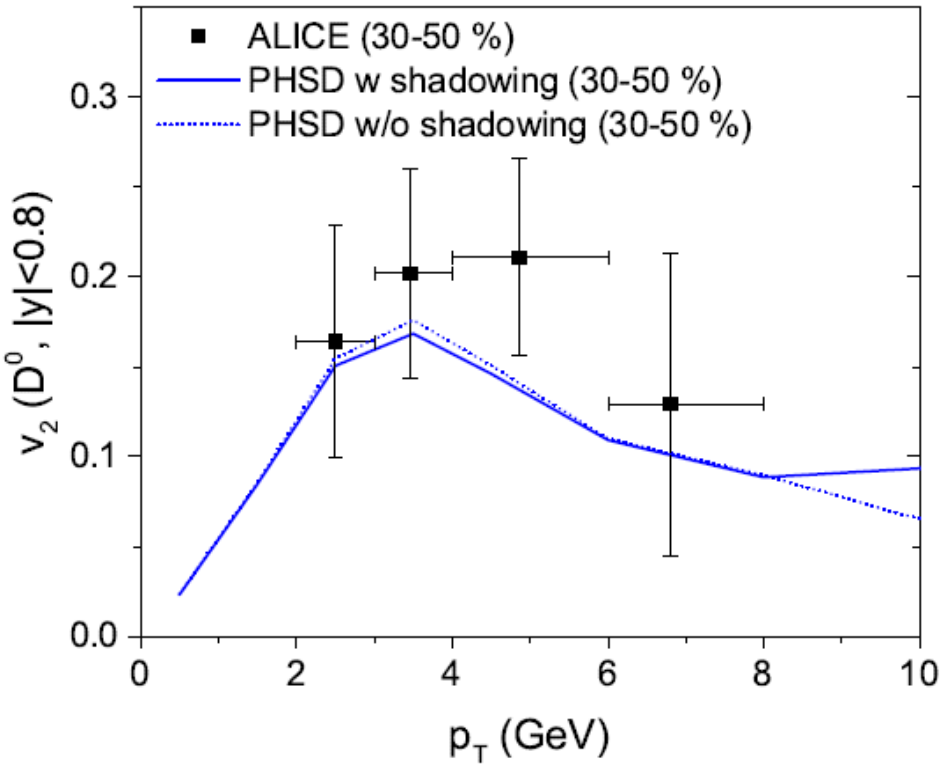

- Shadowing effect has small impact on v_2
- Hadronic rescattering increases v_2

T. Song et al., arXiv:1512.0089

Off-shell effect for charm in QGP: cross sections

Note: the spectral function of c (cbar) quarks cannot be fitted from lattice QCD data due to their small contribution to the entropy

Compare two scenarios for m_C (light quarks are off-shell!):

1) m_C=1.5 GeV
2) m_C = off-shell with the same width of s.f. as for the light quarks

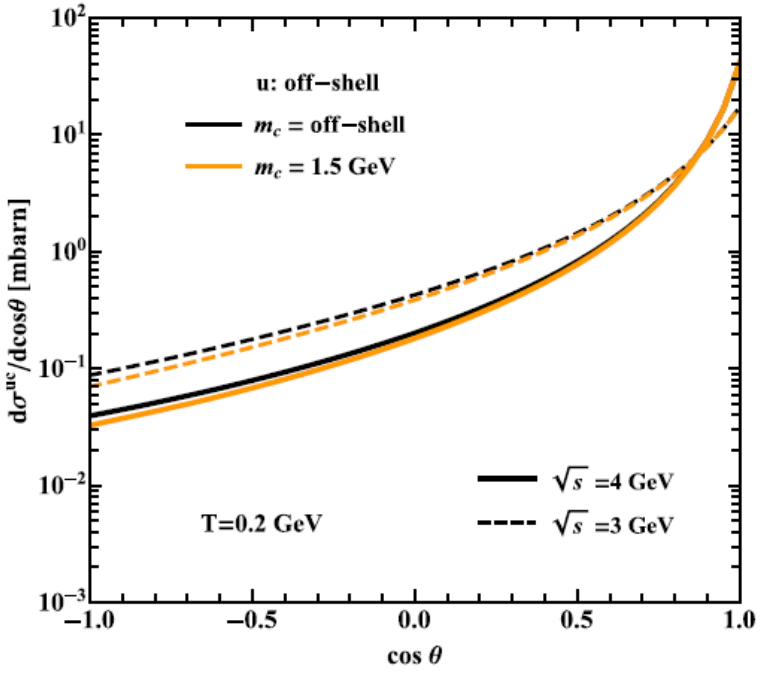

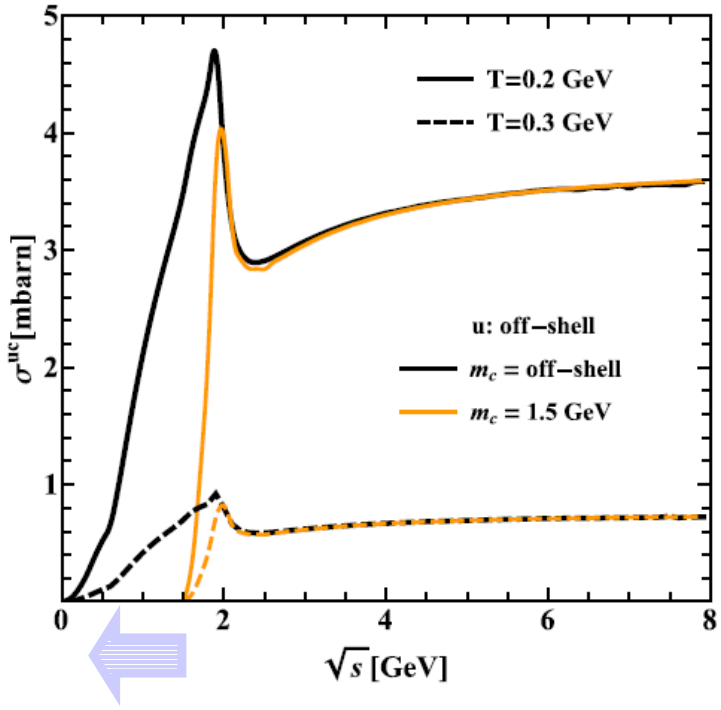

- Differential elastic cross section for uc→uc: small effect from off-shellness
- Total elastic cross section for uc→uc: big effect : shift of threshold to low $s^{1/2}$

T. Song et al., arXiv:1512.0089

Off-shell effect for charm in QGP: thermal properties

Compare two scenarios for m_C (light quarks are off-shell!):

1) m_C=1.5 GeV
2) m_C = off-shell with the same width of s.f. as for the light quarks

Charm collisional energy loss as a function of the c-quark momentum

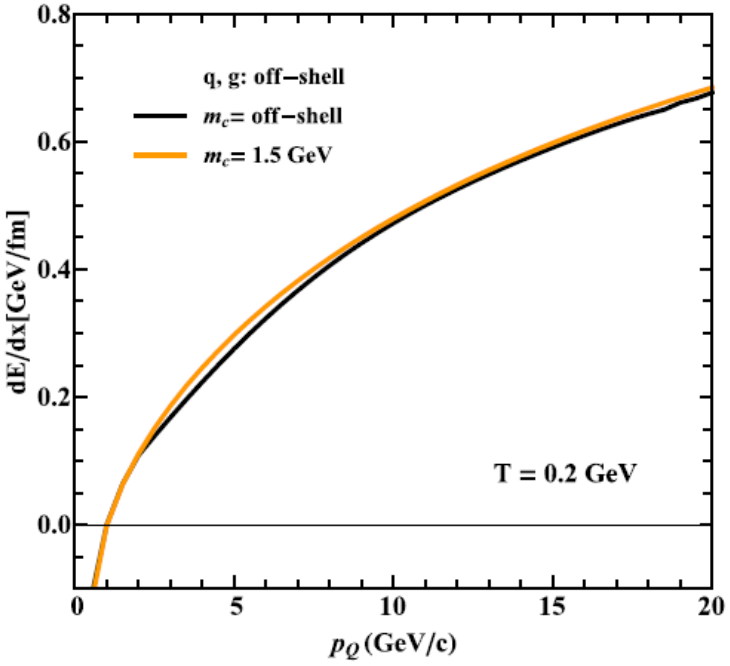

Spatial diffusion constant D_s as a function of medium temperature

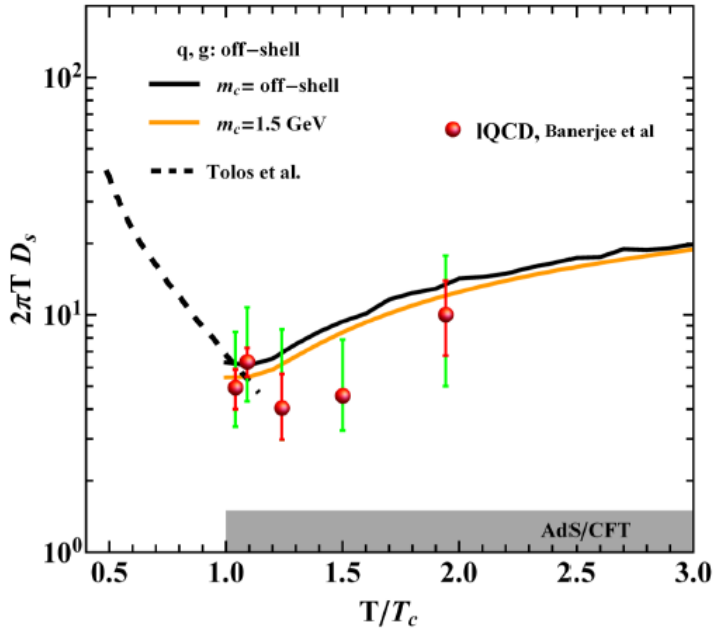

For the QGP in equilibrium:
the off-shellness effect on charm energy loss and D_s is moderate

T. Song et al., arXiv:1512.0089

Off-shell effect for charm R_{AA} and v_2 at LHC

HIC: off-equilibrium → potential becomes important due to the large gradients in density

Quark spectral function with width

Components: time like & space like

partons

potential energy

scalar + vector

- **Scalar potential density increses with T and gives repulsive force on partons in HIC (except nea T_C due to hadronization) → dominant at HIC**

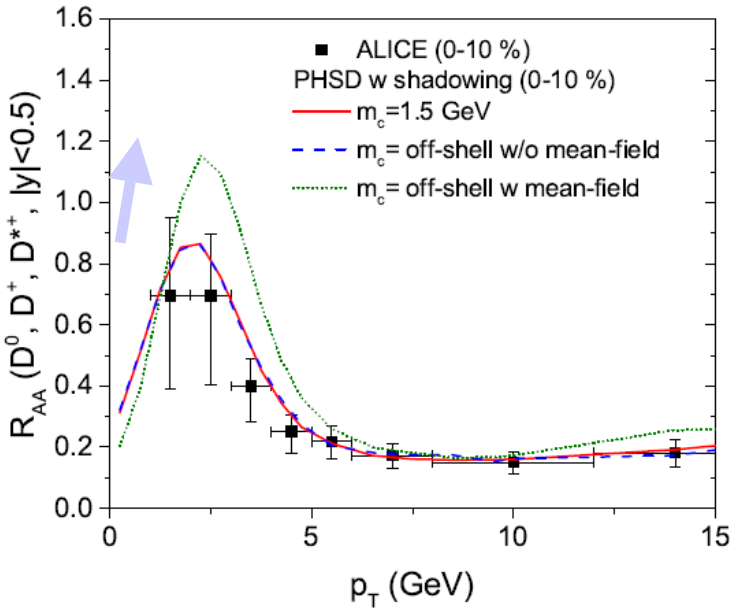

Charm scalar repulsive forces are unknown:
Assumpion to investigate – use for charm the same forces as for light quark!

- **Finding from HIC: PHSD vs exp. data →**
  1) The effect of off-shell charm without repulsive force on R_{AA} and v_2 is small
  2) ALICE data favors a weaker repulsive force for off-shell charm quarks compared to light quarks.

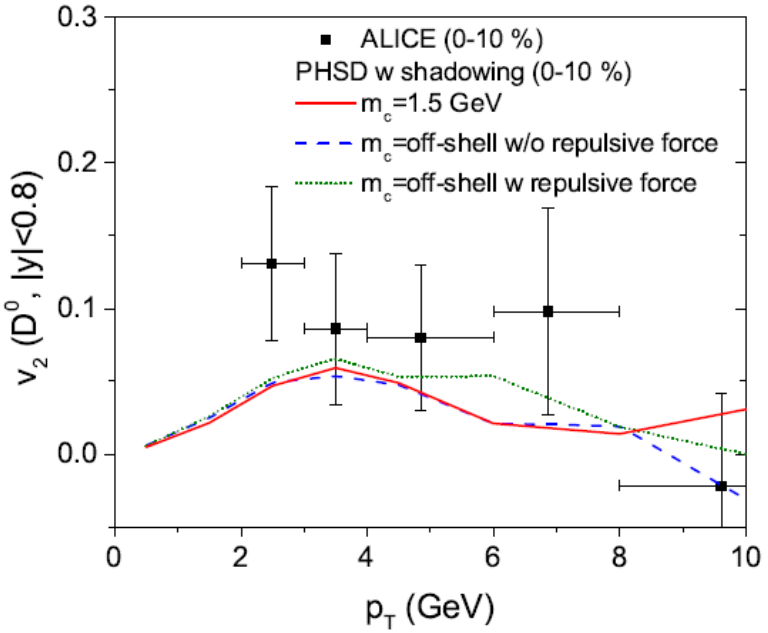

T. Song et al., arXiv:1512.0089

Summary

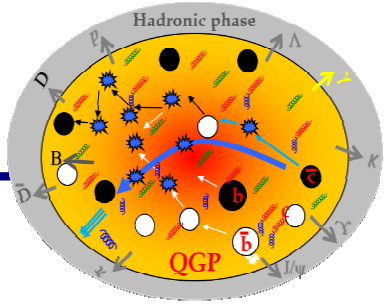

- PHSD provides a microscopic description of non-equilibrium charm dynamics in the partonic and hadronic phases

- Partonic rescattering suppresses the high p_T part of R_{AA}, increases v_2
- Hadronic rescattering moves R_{AA} peak to higher p_T, increases v_2

- The structure of R_{AA} at low p_T is sensitive to the hadronization scenario, i.e. to the balance between coalescence and fragmentation
- Shadowing effect supresses R_{AA}

- The exp data for the R_{AA} and v_2 at RHIC and LHC are better described in the PHSD:

  by QGP collisional energy loss due to the elastic scattering of charm quarks with massive quarks and gluons in the QGP phase

  + by the hadronization scenario „coalescence with <r>=0.9 fm + fragmentation“

  + by strong hadronic interactions due to the elastic scattering of D,D* mesons with mesons and baryons

Outlook

- the BES RHIC – in progress
- Influence of radiative energy loss at larger p_T ?

(expected to be strongly suppressed at lower transverse momenta in the PHSD due to the large mass of gluons for lower relative momenta)

Thank you!

Energy loss

H. Berrehrah et al, PRC 91 (2015) 054902

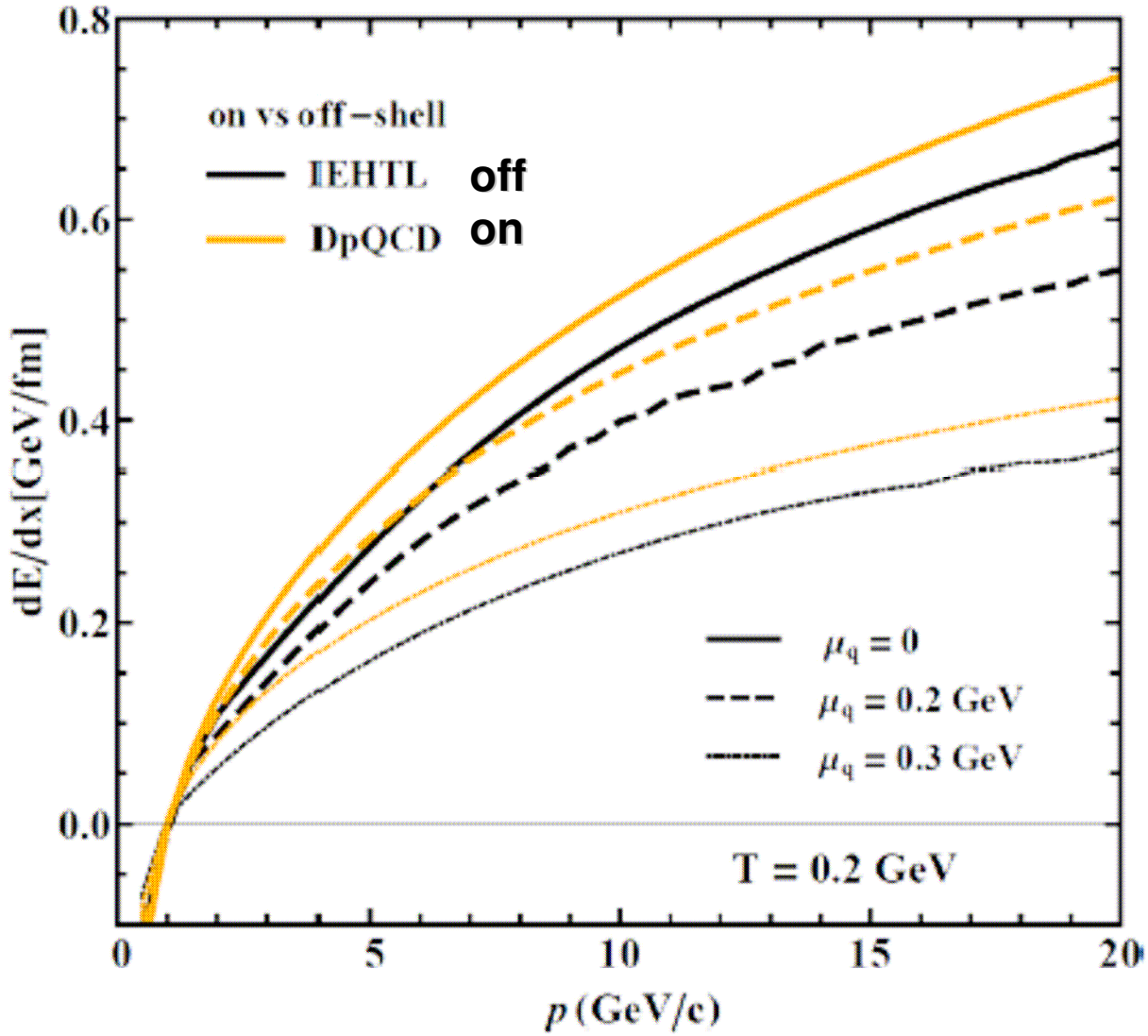

Longitudinal and transverse momentum change

H. Berrehrah et al, PRC 91 (2015) 054902

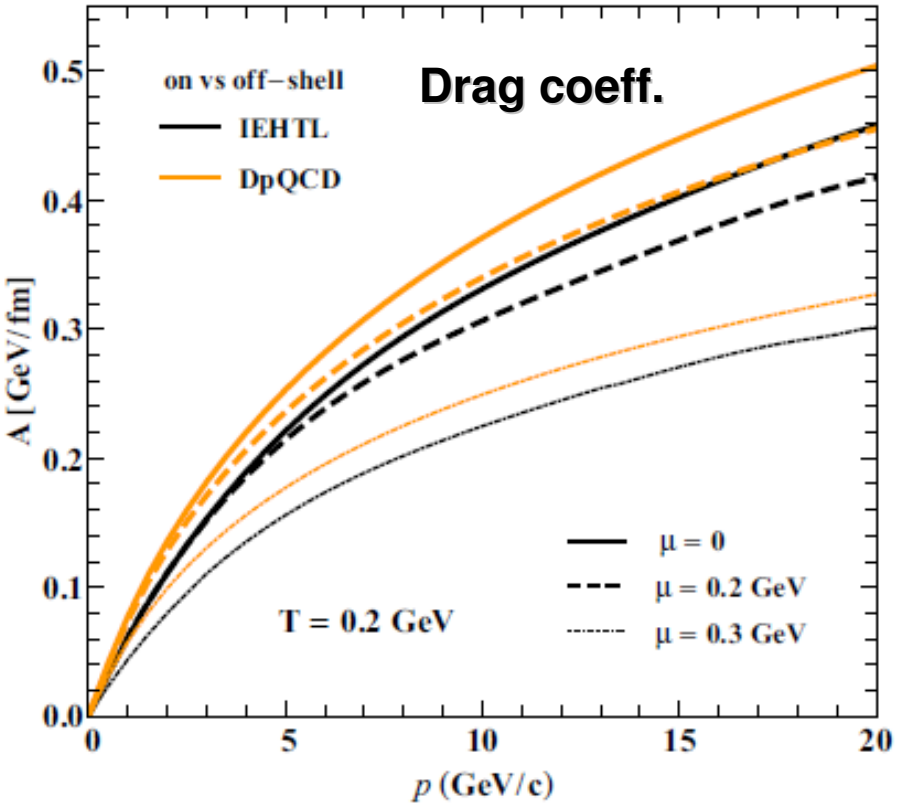

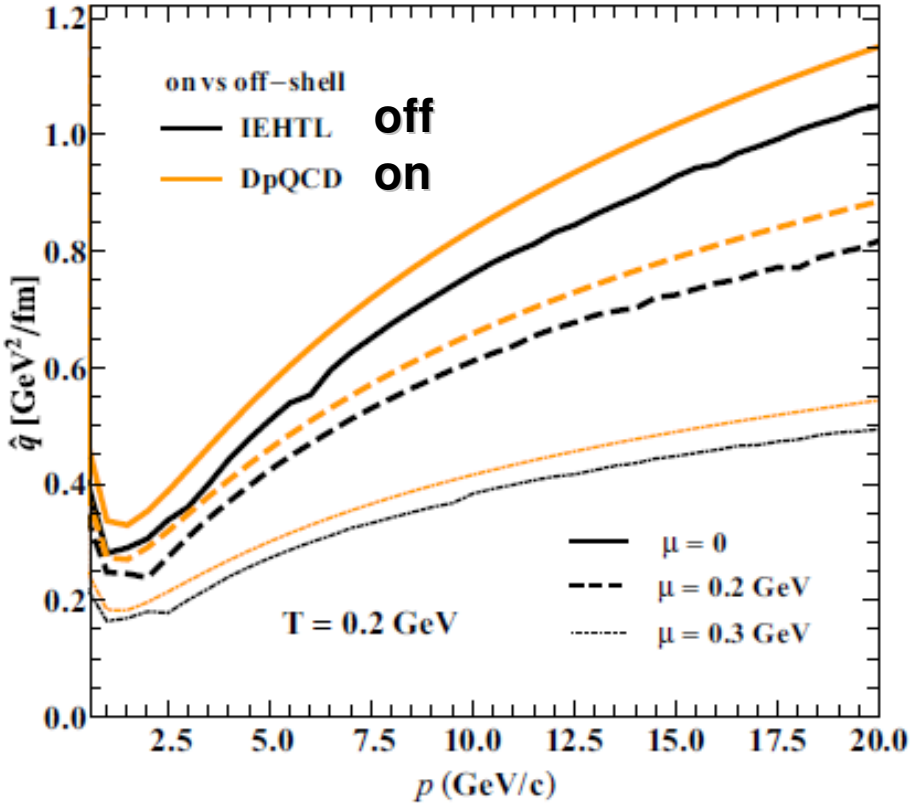

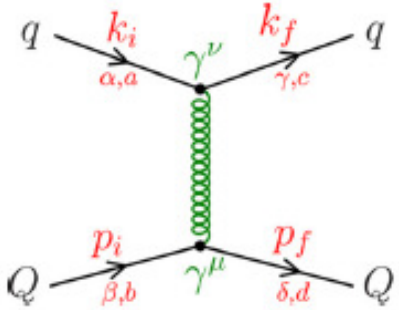

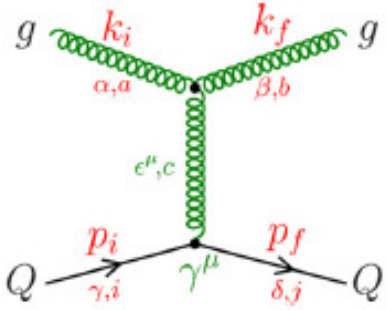

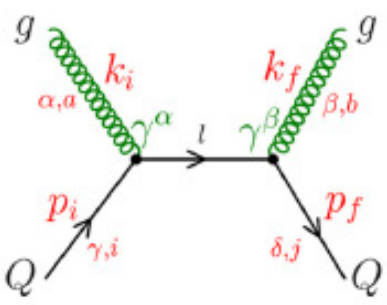

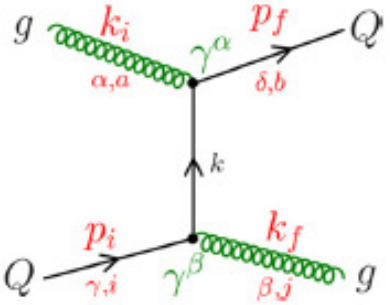

Transverse momentum change in DQPM

$$\hat{q}^{\rm off}(p,T,\mu_q) = \frac{1}{2(2\pi)^3}\Pi_{i\in p,q,p',q'}\int \frac{m_p^2}{p} m_i dm_i \rho_p^{\rm BW}(m_i) \times \int \frac{q^5 m_p}{s^2 E_q}\left[\frac{m_1^{\rm off}(s)-m_2^{\rm off}(s)}{2}(f_0+f_2) + \frac{(E_q+m_p)^2}{s} m_2^{\rm off}(s)(f_0-f_2)\right] dq, \quad (6.6)$$

with

$$m_2^{\rm off}(s) = \frac{1}{8p^i p^f}\int_{t_{\rm min}}^{t_{\rm max}} \frac{1}{g_g g_Q}\sum_{ij}\sum_{kl}|\mathcal{M}^{\rm off}|^2(s,t;i,j|l,k) \times\left[1-\frac{t-\left(M_Q^i\right)^2+\left(M_Q^f\right)^2-2E^iE^f}{2p^ip^f}\right]^2 dt.$$

$$m_1^{\rm off}(s) := \frac{1}{4p^ip^f}\int_{t_{\rm min}}^{t_{\rm max}} \frac{1}{g_p g_Q}\sum_{i,j}\sum_{k,l}\left|\mathcal{M}_{2,2}^{\rm off}(s,t;i,j|k,l)\right|^2 \times\left[1-\frac{t-\left(M_Q^i\right)^2+\left(M_Q^f\right)^2-2E^iE^f}{2p^ip^f}\right] dt,$$

$$f_n(q) = \frac{1}{2}\int d\cos\theta_r\; f\left(\frac{u^0E_q - uq\cos\theta_r \mp \mu_q}{T}\right)\cos^n\theta_r.$$

$$\langle|\mathcal{M}|^2\rangle = \frac{1}{4}\sum_{\rm spins} T_{\alpha\beta}T^{\star}_{\alpha'\beta'}\varepsilon_i^{\alpha}\varepsilon_i^{\star\alpha'}\varepsilon_f^{\beta}\varepsilon_f^{\star\beta'},$$

$$\sum|\mathcal{M}|^2 = \frac{2g^4}{9\left[\left(t-m_g^2\right)^2+4\gamma_g^2q_0^2\right]} \times\left[4\left(p_f^\mu p_i^\nu + p_i^\mu p_f^\nu + g^{\mu\nu}\frac{t}{2}\right)\right] \times\left[4\left(k_{f,\mu}k_{i,\nu}+k_{i,\mu}k_{f,\nu}+g_{\mu\nu}\frac{t}{2}\right)\right],$$

H. Berrehrah et al, PRC 91 (2015) 05490

DQPM: on-shell vs off-shell

H. Berrehrah et al, PRC 89 (2014) 054901;
PRC 90 (2014) 051901; PRC90 (2014) 064906;
PRC 91 (2015) 054902

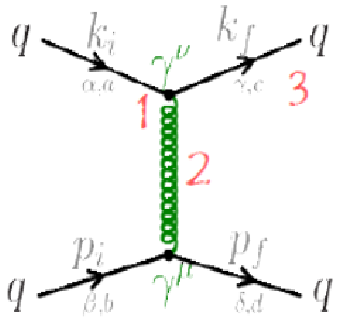

1. α_s at finite (T, μ)
2. Propagator $G^{\mu\nu}$ and "IR" at finite (T, μ)
3. $m_{q,\bar{q},g}$ at finite (T, μ)

- DpQCD (Dressed pQCD) : On-shell non-pQCD
  - $\alpha_s^{DQPM}(T,\mu)$, IR, m : from DQPM (DQPM pole mass for g, q, $\bar{q}$)
  - $G^{\mu\nu}(q, m_g) = -i\dfrac{g_{\mu\nu} - q_\mu q_\nu / m_g^2}{q_0^2 - \boldsymbol{q}^2 - m_g^2}$
- IEHTL (Infrared Enhanced HTL) : Off-shell non-pQCD
  - $\alpha^{DQPM}(T,\mu)$, IR, m, ρ^{BW} from DQPM (finite mass and width)
  - Off-shell kinematical limits
  - $G^{\mu\nu}(q, m_g) = -i\dfrac{g_{\mu\nu} - q_\mu q_\nu / m_g^2}{q_0^2 - \boldsymbol{q}^2 - m_g^2 + i2\gamma_g q_0}$
  - $\sigma^{IEHTL}(s,T) = \int \Pi dm^{(i)}\ \sigma^{q,g-Q}(s, m^{(1)}, m^{(2)}, m^{(3)}, m^{(4)})\ \rho_{(1)}(m^{(1)})\ \rho_{(2)}(m^{(2)})\ \rho_{(3)}(m^{(3)})\ \rho_{(4)}(m^{(4)})$

Phys.Rev. C89, 054901 (2014)
J. Phys. : Conf.Ser. 509 012076,
arXiv :1405.3243, arXiv :1406.5322